DEVELOPING A METHOD TO ESTIMATE THE WATER USE OF SOUTH AFRICAN NATURAL VEGETATION USING REMOTE SENSING

MR Ramjeawon

Submitted in fulfilment of the requirements

for the degree of MSc Hydrology

Centre for Water Resources Research

School of Agriculture, Earth and Environmental Sciences

University of KwaZulu-Natal

Pietermaritzburg

South Africa

December 2016

ABSTRACT

The scarcity of water is a growing concern throughout the world. It is essential to accurately determine the quantity and quality of this valuable resource to aid in water resource planning and management. For this purpose a hydrological baseline is required to compare against the water use of other land uses. Currently, the Acocks (1988) Veld Type is the baseline land cover used for hydrological studies. However, there are several shortcomings associated with this baseline land cover that may be overcome by using the recently released natural land cover map produced by South African National Biodiversity Institute (SANBI) 2012.

A barrier to the use of the SANBI (2012) vegetation map is that, the water use parameters have not been determined for the various vegetation units defined. Vegetation water use can be determined by estimating the total evaporation (ET). There are a number of *in-situ* methods available to estimate ET. However, these methods estimate ET based on point or line averaged measurements which are only representative of local scales and cannot be extended to large areas because of land surface heterogeneity. The application of remote sensing energy balance models has the potential to overcome these limitations. Remote sensing has the ability to produce large spatial scale estimates of ET. It can also provide information at remote sites where it is difficult to install instruments.

The focus of this study was to develop a method to estimate ET for natural vegetation of South Africa using remote sensing. The Surface Energy Balance System (SEBS) model in conjunction with Landsat 7 ETM+ and 8 OLI/TRS images was first used to validate point-based ET from various biomes across the country. The results from the study indicate a fair comparison between the *in-situ* ET data and the evaporation estimates produced using the SEBS model with coefficient of determination value of 0.66 being achieved and a RMSE of 1.74 mm.day^{-1}. The highest RMSE was attained for the Ingeli forest site whilst the lowest belonged to the Nama Karoo site of 2.2 mm.day^{-1} and 0.5 mm.day^{-1}, respectively. The SEBS model was able to estimate ET which mimics the trend of *in-situ* ET well. However, the model tends to over-estimate ET in comparison to *in-situ* ET data. Following the validation of the *in-situ* and SEBS ET, the SEBS model was applied to model ET for a year. For this investigation, cloud free Landsat 8 OLI/TRS images was obtained for each biome for the period between 1 July 2014 to 31 June 2015. The highest ET value of 8.7 mm/day was obtained from the Forest biome on the 12 January 2015 and the lowest ET estimate of 0.09 mm/day was on the 17 January 2015 for the Nama Karoo biome. The Forest biome recorded

the highest mean ET value of 4.9 mm/day whilst the lowest mean ET value was 0.71 mm/day attained from the Nama Karoo biome.

Satellite derived ET using the SEBS model produced reliable estimates when compared to *in-situ* ET. The spatial and temporal resolution of ET can be achieved using remote sensing. The ET estimates from SEBS compared well to the *in-situ* ET measurements and followed the seasonal trend, however an over-estimation of ET was present in some cases. Overall, remote sensing proves a viable option to estimate ET over large areas. This method can be applied to derive the water use which can be used to determine water use parameters.

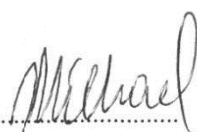# DECLARATION - PLAGIARISM

I, Manish Ramjeawon declare that:

(i)   The research reported in this thesis, except where otherwise indicated, is my original work.

(ii) This thesis has not been submitted for any degree or examination at any other university.

(iii) This thesis does not contain other persons' data, pictures, graphs or other information, unless specifically acknowledged as being sourced from other persons.

(iv) This thesis does not contain other persons' writing, unless specifically acknowledged as being sourced from other researchers. Where other written sources have been quoted, then:

(a) Their words have been re-written but the general information attributed to them has been referenced;

(b) Where their exact words have been used, their writing has been placed inside quotation marks, and referenced.

(v)   Where I have reproduced a publication of which I am an author, co-author or editor, I have indicated in detail which part of the publication was actually written by myself alone and have fully referenced such publications.

(vi) This thesis does not contain text, graphics or tables copied and pasted from the Internet, unless specifically acknowledged, and the source being detailed in the thesis and in the References sections.

Signed: ....

Manish Ramjeawon

Supervisor: ....

Dr. ML Warburton Toucher

Co-supervisor: ....

Dr. M Mengistu

PREFACE

The work described in this dissertation was carried out in the Centre for Water Resources Research, School of Agriculture, Earth and Environmental Sciences, University of KwaZulu-Natal, Pietermaritzburg under the supervision of Dr. Michele Warburton Toucher and Dr. Michael Mengistu.

The research represents original work by the author and has not otherwise been submitted in any form for any degree or diploma to any tertiary institution. Where use has been made of the work of others it is duly acknowledged in the text.

ACKNOWLEDGEMENTS

DEDICATION

To my parents and grandparents

TABLE OF CONTENTS

x

LIST OF FIGURES

LIST OF TABLES

LIST OF ABBREVIATIONS

AET   Actual Evapotranspiration

ASTER   Advanced Space-borne Thermal Emission and Reflection Radiometer

BREB   Bowen Ratio Energy Balance

CWSI   Crop Water Stress Index

DEM   Digital Elevation Model

EF   Evaporative Fraction

ET   Total Evaporation

ET_c Evapotranspiration of a Crop

ET_o Reference Crop Evapotranspiration

ET_rF Fraction of Reference Evapotranspiration

G_o Soil Heat Flux

GIS   Geographic Information System

H   Sensible Heat Flux

K_c Crop Coefficient

LAI   Leaf Area Index

LE   Latent Heat Flux

METRIC   Mapping Evapotranspiration with Internalised Calibration

MODIS   The Moderate-Resolution Imaging Spectro-radiometer

NDVI   Normalised Difference Vegetation Index

NWA   National Water Act

PET   Potential Evapotranspiration

RMSE   Root Mean Square Error

SEBAL   Surface Energy Balance Algorithm for Land

SEBS   Surface Energy Balance System

SSEBop   Operational Simplified Surface Energy Balance

SFRA   Streamflow Reduction Activity

SLS   Surface Layer Scintillometer

USGS   United States Geological Survey

VITT   Vegetation Index Surface Temperature Triangle/Trapezoidal Model

WDI   Water deficit index

LIST OF SYMBOLS

Rn   Net radiation (W.m^{-2})

G$_o$ Soil heat flux (W.m^{-2})

H   Sensible heat flux (W.m^{-2})

λE   Latent heat flux (W.m^{-2})

$\propto s$ Shortwave albedo

R$_s$ Shortwave radiation (W.m^{-2})

ε_s Surface emissivity

ε_a Atmospheric emissivity

T$_a$ Air temperature (K)

T$_s$ Surface temperature (K)

σ Stefan-Blotzman constant (5.67x10^{-8} W.m$^{-2.}$K^{-4})

c_p Specific heat of air (MJ.kg-$^{1.o}$C^{-1})

T$_o$ Aerodynamic temperature (K)

T$_a$ Air temperature (K)

r$_a$ Aerodynamic resistance (s.m^{-1})

r$_s$ Surface resistance (s.m^{-1})

γ Psychrometric constant (k.Pa.^{o}C^{-1})

ρ_a Density of air (kg.m^{-3})

E$_{daily}$ Actual daily evaporation (mm.day^{-1})

ρ_w Density of water (kg.m^{-3})

$(T_s-T_a)_{max}$ Maximum surface and air temperature (K)

$(T_s-T_a)_{min}$ Minimum surface and air temperature (K)

M_a Soil moisture availability index

R_{lwd} Longwave radiation (W.m^{-2})

$\propto$ Albedo

fc Fractional canopy coverage

H_{dry} Sensible heat flux at dry limit (W.m^{-2})

H_{wet} Sensible heat flux at wet limit (W.m^{-2})

$L\lambda$ Radiance (W.(m^{-2}.sr^{-1}.μm))

$\rho\lambda$ Top of atmosphere reflectance

n Sunshine duration (hours)

N Maximum duration of sunshine (hours)

R_a Extraterrestrial radiation (MJ.m-^{2}day^{-1})

G_{sc} Solar constant of (0.0820 MJ.m^{-2}min^{-1})

d_r Inverse relative Earth-Sun distance (radians)

ω_1 and ω_2 Solar time angle at the beginning and end of the period (radians)

φ Latitude of the site (radians)

δ Solar declination (radians)

1. INTRODUCTION

1.1 Background

In many semi-arid countries, such as South Africa, water is a scarce commodity (Gibson *et al.,* 2013). Added to this are the impacts of population growth, land use and climate change on water (Schulze, 2003; Warburton *et al*., 2010). As a result, water resources management has become critical and requires an in-depth understanding of the hydrological cycle and processes, as well as the impacts on these (Warburton *et al*., 2010; Warburton *et al.,* 2011). To ensure that water is used efficiently and effectively, decisions pertaining to water resources need to be well-informed and based on the best available information.

The land cover and land use has been significantly altered over time to meet the demands of the growing population. The partitioning of rainfall into various components such as groundwater recharge, surface runoff, total evaporation and infiltration have been altered by land use change (Falkenmark *et al.,* 1999; Costa *et al.,* 2003). Given the sensitivity of the hydrological responses to changes in land use, it is essential that accurate estimates of the impacts of land use on water availability, use and allocation can be made. In order to make these estimates, a reference land cover or baseline is required against which the response changes can be assessed (Schulze and Pike, 2004; Jewitt *et al.,* 2009; Gush, 2010). The reference or baseline land cover that is used will determine the magnitude of the impact of land use on the hydrological responses. Thus, to achieve accurate estimates of the impacts of land use, an accurate baseline and knowledge of its water use is required. In South Africa, the National Water Act of 1998 (NWA, 1998) requires reference flows to determine the ecological reserve and assess the impact of various land uses on low flows. Therefore, the need for an accurate reference or baseline land cover has become more important.

Currently, the Acocks' (1988) Veld Types are regarded and accepted by the Department of Water and Sanitation, as well as others, as the baseline vegetation for South Africa (Schulze, 2007; Jewitt *et al.,* 2009). A Veld Type is described as an array of vegetation with a variation that is small enough to consider it all the same (Acocks, 1953). Acocks' (1988) states that a Veld Type "is based on a major indicator species within it, is a manageable unit at local, regional and national scale and is based on the separation of natural variation of vegetation types from variations induced by human influences" (Shulze, 2007:2). The various vegetation

1

types were grouped into manageable units, which produced the 70 different veld types. Not every area of the country was covered in equal detail by Acocks (1953). The western half, Lesotho and the former north-western Transvaal areas were mapped in less detail than the eastern region (Acocks, 1953). The Acocks' Veld Type maps were updated in 1975 and 1988 with photographs and plant names (Mucina and Rutherford, 2006). It was produced at a country-wide scale and displayed little detail at local scale. Additionally, when the Acocks' (1988) Veld Types were parameterized for use in a hydrological model few studies had been conducted to assess the water use of natural vegetation. Therefore, little to no information was available to confirm these values (Jewitt *et al.,* 2009).

With the release of the Mucina and Rutherford (2006) natural vegetation map, which was updated to the SANBI (2012) vegetation map, the opportunity emerged to address some of the concerns around using the Acocks' (1988) Veld Types as a baseline land cover. The natural vegetation map produced by SANBI (2012) defines approximately 450 vegetation units, based on improved mapping using spatial predictive modelling, satellite imagery, large databases and aerial photographs in combination with traditional field-based data. A vegetation unit is defined as "a complex of plant communities ecologically and historically (both in spatial and temporal terms) occupying habitat complexes at the landscape scale" (Mucina and Rutherford, 2006: 16). The vegetation units were formed using the following criteria: location along dominant ecological gradients, dominant ecological factor at landscape level, dominant vegetation structure, high level of floristic similarity, close proximity and potential (Mucina and Rutherford, 2006). The SANBI (2012) natural vegetation map provides greater detail at local scale compared to the Acocks' (1988) Veld Types and includes areas which were poorly mapped by Acocks' (1988) Veld Types. This, together with the growing body of literature on natural vegetation water use, and the application of remote sensing estimates means that the accepted baseline against which the impacts of land use change on the hydrological response are assessed can be improved. With the improved spatial detail in the natural vegetation mapping and having a greater understanding of the natural vegetation water use, the determination of reference flows can be undertaken with better accuracy.

This research project forms part of a larger Water Research Commission (WRC) funded project titled "Resetting the baseline land cover against which streamflow reduction activities and the hydrological impacts of land use change are assessed" (Report No. K5/2437). There

were a number of aims outlined in the proposal. The first aim was to cluster the vegetation units, using the SANBI (2012) natural vegetation, into hydrologically relevant groupings. This was done using climatic, vegetation and landscape characteristics. The second aim of the WRC project was to determine the water use of the vegetation clusters. This Masters Research project focused on developing an approach that can be adopted to estimate the water use of the vegetation clusters. The SANBI (2012) vegetation map used in the clustering of the vegetation units was used in this study. The water use will aid in determining the crop coefficient required as an input in a hydrological model, which is the third aim of the WRC project.

The measurement of total evaporation (ET) can be used to determine the water use of vegetation. Verstraeten *et al.* (2008) provided a comprehensive review on the different methods used to estimate ET, which included the Bowen ratio (Fristchen and Simpson, 1989), surface renewal (Paw U *et al*., 1995; Snyder *et al*., 1996), scintillometer (Hill, 1992; Thiermann and Grassl, 1992; de Bruin *et al*., 1995), lysimeters and eddy covariance (Meyers and Baldocchi, 2005). These are *in-situ* methods which estimate ET by determining the different components of the energy balance using point or line averaged measurements. However, the *in-situ* methods estimate ET at a small scale (< 5 km) and are limited due to land surface heterogeneity (French *et al., 2005). In-situ* instruments cannot be located at sites which are hard to access therefore limiting the measurement of ET in these areas. These methods are, in some cases, costly and require maintenance. In the context of this study, the water use from SANBI (2012) natural vegetation map was required at a national scale similar to the scale the water use from the clusters will need to be determined. Therefore a more broad modelling approach to estimate ET was required.

The advent of remote sensing overcomes many of the challenges experienced by *in-situ* techniques. Remote sensing of ET can be used to provide data at local, catchment and regional scale. The difficultly to capture land surface heterogeneity of vegetation is overcome using remote sensing (Allen *et al., 2007). Remote sensing techniques can be cost effective and provide information on ET in areas which are difficult to access using *in-situ* techniques. There are a number of remote sensing models available to estimate ET. The models vary in complexity and are selected based on the requirement of the study. For large scale estimates, satellite remote sensors are ideal. Given that remote sensing overcomes the challenge of spatial scale as well as other challenges experienced with *in-situ* methods, it was selected to

estimate ET for the SANBI (2012) natural vegetation. The SANBI (2012) natural vegetation map consists of approximately 450 vegetation units. However, it was impractical to determine the water use at such a fine scale. Therefore for the purpose of this study the SANBI (2012) biomes were used. The biomes reflect a simplified unit which consists of vegetation units which are similar in structure, macroclimate and are exposed to similar characteristics of disturbance for example, fire and grazing (Mucina and Rutherford, 2006).

1.2 Aims and Objectives

The aim of this research was to develop a method to estimate the ET of natural vegetation in South Africa using remote sensing. The method is to be adopted to determine the water use of the vegetation clusters units. The SANBI (2012) land cover map of natural vegetation for South Africa was used as it provides more detail of natural vegetation and was used to determine the vegetation clusters.

The specific objectives of this study were to:

- Review a number of remote sensing techniques available to estimate ET.
- Validate the selected technique (SEBS model) against *in-situ* ET at sites located in the Grasslands, Savanna, Fynbos, Forest, Albany Thicket, Indian Ocean Coastal Belt and Nama Karoo biomes.
- Use SEBS to model ET for a year to provide spatial and temporal variations of ET across the different biomes.

The research questions were:

i. How do the SEBS estimates of ET for natural vegetation compare to *in-situ* ET measurements over natural vegetation?
ii. How does ET vary (seasonally and spatially) between the various South African biomes?
iii. Is remote sensing a suitable approach to determine the water use of the vegetation clusters?

1.3 Dissertation Outline

The dissertation has been written as a traditional monologue. Following this introduction, Chapter Two presents a comprehensive literature review which describes total evaporation and the surface energy balance. The various direct and indirect methods to estimate ET are reviewed in detail including both the advantages and disadvantages. This is followed by an evaluation of the common remote sensing ET models applied in South Africa. The Surface Energy Balance System (SEBS) model is discussed in detail with examples of its application in South Africa. Following this, Chapter Three outlines the methodology followed. The chapter details the study site, satellite and meteorological data acquisition, the setting up and application of the SEBS model to estimate ET for the various biomes. The results are presented in Chapter Four for both the validation study and the modelled ET produced from SEBS. A discussion is provided in Chapter Five prior to the conclusion, limitations and recommendations being given in Chapter Six.

2. LITERATURE REVIEW: DETERMINING THE WATER USE OF NATURAL VEGETATION

Natural vegetation are plants, belonging to various species, which compete, live and assist each other in a particular habitat without human influence (Acocks, 1953). The water use from natural vegetation can be determined by measuring total evaporation (ET). ET is defined as the loss of water from the earth's surface to the atmosphere (Jovanovic *et al.,* 2011). The various direct and indirect methods used for estimating latent energy flux and ET are described in this chapter. Amongst those are a number of remote sensing based models that vary in complexity to estimate ET at large scales. The micrometeorological, evapotranspiration models and remote sensing models to estimate ET are discussed. Total evaporation estimation using the shortened surface energy balance equation are discussed in the section which follows.

2.1 Total Evaporation and the Surface Energy Balance

The term total evaporation (ET) is used to estimate vegetation and crop water use. It is the combined process of transpiration, evaporation and interception (Al-Kaisi and Broner, 2009). Evaporation is the loss of water via a water body, soil surface and interception (Allen *et al.,* 1998). There are a number of climatic factors, which influence the rate and amount of water evaporated. These include solar radiation, humidity, precipitation, air temperature and wind speed (Allen *et al.*, 1998). Transpiration is the loss of water via the stomata of plants, whereby vaporization occurs within the plant tissues and water is lost to the atmosphere (Allen *et al.*, 1998). The main driving factor is solar radiation followed by air temperature (Allen *et al.*, 1998).

ET is the second largest component in the hydrological cycle, following precipitation (Van der Tol and Parodi, 2011). To estimate ET the effects of energy and water are observed (Van der Tol and Parodi, 2011). The energy balance equation is used to determine latent energy flux (λE), which is described, as the energy consumed during evapotranspiration (Van der Tol and Parodi, 2011). To determine ET, the energy balance is rearranged to estimate λE, as shown in Equation 2.1.

$$\lambda E = R_n - G - H \tag{2.1}$$

where, R_n is the net radiation (W.m^{-2}), G_o is the soil heat flux (W.m^{-2}), H is sensible heat flux (W.m^{-2}) and λE is the latent heat flux (W.m^{-2}).

R_n, G_o and H can be determined, using remote sensing albedo, radiometric surface temperature, using the thermal, visible and near infrared bands in conjunction with meteorological data, such as wind speed, relative humidity, air temperature and solar radiation (Li *et al.,* 2009). R_n is the total energy which is partitioned into G_o, H and λE (Li *et al.,* 2009). R_n is defined as:

$$\tag{2.2}$$

$$R_n = S_N + L_N$$

where S_N is net shortwave radiation (W.m^{-2}) and L_N is net long wave radiation (W.m^{-2})

which translates to:

$$R_n = (1 - \propto_s)R_s + \varepsilon_a \sigma T_a^4 - \varepsilon_s \sigma T_s^4 \tag{2.3}$$

where $\propto_s$ is the shortwave albedo, R_s is the downward shortwave radiation (W.m^{-2}), ε_a is the atmospheric emissivity, T_a is air temperature (K), T_s is surface temperature (K) and σ is the Stefan-Blotzman constant (5.67×10^{-8}) in W.m$^{-2.}$K^{-4}.

The soil heat flux (G_o) can be defined as the heat energy used to warm or cool a volume of soil via a loss of heat (Li *et al.,* 2009). It is directly related to the temperature gradient and thermal conductivity with the depth of the top soil and is conventionally estimated using sensors inserted into the soil (Li *et al.,* 2009). G_o is defined as:

$$G_o = G_{plate} + G_{stored} \tag{2.4}$$

where G_{plate} is measured using a soil heat flux plate. G_{stored} is defined as the energy stored above the soil heat flux plates. It is determined using the change in soil temperature at two depths, soil bulk density, the specific heat capacities of soil and water and volumetric soil water content.

The sensible heat flux (H) is the energy used to warm or cool the air (Li *et al.,* 2009). It can be determined by combining the difference of aerodynamic and air temperature with the aerodynamic resistance, as defined below:

$$H = \frac{\rho_a c_p (T_o - T_a)}{r_a} \qquad (2.5)$$

where ρ_a is density of air (kg.m^{-3}), c_p is specific heat capacity of air at constant pressure (J.kg^{-1}.K^{-1}), T_o is aerodynamic temperature, T_a is air temperature (K) and r_a is aerodynamic resistance (s.m^{-1}).

The accuracy of λE is dependent on precise measurement of the R_n, G_o and H (Allen *et al.,* 1998). R_n, G_o and H can be measured, using ground-based and remote sensing methods. The common ground-based instruments used to determine R_n is the net radiometer. G_o is determined using the soil heat flux plates, soil temperature probes and volumetric water content sensors. The most difficult parameter to measure in the energy balance equation is H (Van der Tol and Parodi, 2011). Section 2.2 describes a number of methods available to determine H and ET.

2.2 Direct and Indirect Methods to Estimate Total Evaporation

The following section covers a range of instruments used to measure and estimate ET. The methods discussed are micrometeorological techniques, ET estimation models and remote sensing techniques. The micrometeorological techniques are reviewed as the observed ET used in this study was measured using these techniques and the ET estimation models are required to determine the water use parameters. Remote sensing models using the residual of the energy balance approach are discussed as it is the most widely applied method to estimate ET.

2.2.1 Micrometeorological techniques of estimating ET

The micrometeorological techniques comprise of the Bowen ratio, the Eddy covariance, the scintillometer and the surface renewal methods. The Bowen Ratio Energy Balance (BREB), proposed by Bowen in 1926, is the ratio between the sensible and latent heat flux density (Fritschen and Simpson, 1989). The BREB measures vertical fluxes of latent energy and H, producing estimates at the time interval the logger is programmed to (Cook, 2007). Depending on the type used the BREB can be a high maintenance instrument and difficult to set up (Jarmain *et al.*, 2009a). The pumps and motors used to pass air across and alternate the humidity sensor require power, thus influencing the charging and replacement of batteries, thereby increasing the cost. (Jarmain *et al.,* 2009a). The BREB has been successfully used in many applications in South Africa, particularly over grasslands by Everson (2001) and

Savage *et al.* (1997, 2004), forest plantations, such as eucalypts stands, black wattle trees and sugarcane (Jarmain and Everson, 2002; Burger, 1999) as stated by Jarmain *et al.* (2009a).

Reynolds (1895) developed the theoretical framework for the eddy covariance system and the first post-war study was conducted over short vegetation by Swinbank (1951). The Eddy covariance method can estimate λE directly using a sonic anemometer and infrared gas analyser or indirectly by estimating H using a sonic anemometer (and determining λE, using the shortened energy balance equation). The three-dimensional sonic anemometer measures sonic air temperature and three dimensional wind velocities and produces real-time estimates of λE from the covariance between the vertical wind speed and humidity (Meyers and Baldocchi, 2005). H is estimated through the covariance between vertical wind speed and sonic temperature. The estimates of H and λE are point based at a particular height above the vegetation and require a large fetch. The Eddy covariance is a portable instrument, which is capable of recording measurements for long periods (Meyers and Baldocchi, 2005). Savage *et al.* (1997, 2004) has used this method to determine the ET of South African grasslands. One of the disadvantages of the eddy covariance is the lack of energy balance closure when measuring sensible heat and latent heat flux (Savage *et al.*, 2010). The high cost of this instrument is also a disadvantage.

A scintillometer consists of a transmitter and a receiver (De Bruin *et al.,* 1995). The transmitter emits a laser beam, which travels above the canopy. The scintillometer determines H by measuring fluctuations in temperature and humidity (Shuttleworth 2008). The fluctuations are also known as scintillations (Allen *et al.,* 2011). The surface layer scintillometer (SLS) covers a distance between 50-250 m, whereas the large aperture scintillometer is capable of covering a distance between 250 m-5 km (Meijninger *et al.,* 2002).

A scintillometer is easy to operate (Allen *et al.,* 2011) and able to cover small to large ranges (Meijninger *et al.,* 2002). According to Jarmain *et al.* (2009a), the averaging time for the SLS and LAS is much shorter, 1 to 2 minutes compared to the Bowen ratio or Eddy covariance method which is around 20 minutes or longer. The disadvantage of a scintillometer is that it is an expensive instrument (Allen *et al.,* 2011). Added to this, Allen *et al.* (2011) and Savage *et al.* (2004) both explain that the direction of H is not possible using the scintillometer and must be determined by other means. Savage *et al.* (2004) suggest that H can be determined by measuring vertical air temperature, using a pair of thermocouples or an automatic weather

station. Allen *et al.* (2011) and Savage *et al.* (2004) state that the frictional velocity needs to be determined. The scintillometer is dependent on the accurate measurement of R_n and G_o which has to be representative of the entire transect. This is another major uncertainty. The scintillometer signal is strongly weighted to the centre of the transect. The last major disadvantage of the scintillometer is that it is based on an assumption of weak scattering, which does not always occur (Jarmain *et al.,* 2009a). Savage *et al.* (2010) applied the scintillometer over grasslands in South Africa. The scintillometer was used to cover distances ranging from 50 to 101 m (Savage *et al.,* 2010). The ET results obtained compared well to those obtained using the Bowen ratio and Eddy covariance method. The reliability percentage varied between 62 and 85 % (Savage *et al.,* 2010). The lower percentage of reliability was a result of mist and rainfall events which interfered with the beam transmission (Savage *et al.,* 2010). Savage *et al.* (2010) states that the results confirm the reliability of the scintillometer to estimate H.

Paw and Brunet (1991) proposed the surface renewal method which is regarded as a more recent method to determine H compared to the Bowen ratio and Eddy covariance (Mengistu, 2008). The surface renewal method measures air temperature at high-frequency (Snyder *et al.,* 1995), using unshielded fine-wire thermocouples to estimate H (Mengistu and Savage, 2010). Air temperature measurements are recorded between 2-10 Hz (Mengistu and Savage 2010). The surface renewal method is based on the principle that a parcel of air at the surface is replaced by a new parcel of air from above (Snyder *et al.,* 1995). A weighting factor is required to determine H and is obtained using an Eddy covariance (Mengistu and Savage 2010) or literature if available for that vegetation type. The surface renewal method is simple to use, as it requires minimum parameters and is relatively cheap (Mengistu, 2008). The disadvantages associated with the surface renewal method are that it requires a fast responding data logger to record air temperature measurements and the sensors are delicate and easily damaged (Mengistu and Savage 2010). A method to overcome this is to install a number of sensors at the measured location (Mengistu and Savage 2010). Another disadvantage is determining the weighing factor. This is done using an eddy covariance system and is expensive.

2.2.2 Models for estimating evapotranspiration

ET estimation models can be divided into two broad categories *viz.* the analytical approach and the empirical approach. The analytical approach involves, for example, the Food and

Agriculture Organization (FAO) Penman-Monteith, Priestly and Taylor, Shuttle and Wallace model.. The FAO Penman-Monteith is described below. The empirical approach involves the crop coefficient and soil water balance model. The equation was formed, using the energy balance method and the mass transfer method to produce an equation that could determine evaporation from an open water body (Allen *et al.,* 1998). The model was then further developed to take into account surface resistance and aerodynamics, as shown in Equation 2.6 (Allen *et al.,* 1998). The FAO Penman-Monteith equation is used to determine the evaporation from a well-watered grass at a constant height of 0.12 m, an albedo of 0.23 and a surface resistance of 70 m.s^{-1} (Allen *et al.,* 1998). The parameters in Equation 2.6 can be measured or calculated, using weather station data (Allen *et al.,* 1998).

$$\lambda ET = \frac{\Delta(Rn - G) + \rho_a c_p \frac{(e_s - e_a)}{r_a}}{\Delta + \gamma(1 + \frac{r_s}{r_a})} \tag{2.6}$$

where λET is evapotranspiration (mm/day), R_n is the net radiation (MJ.m^{-2}.day^{-1}), G_o is the soil heat flux (MJ.m^{-2}.day^{-1}) e_s - e_a is vapour pressure deficit of the air (kPa), r_a and r_s are the aerodynamic and surface resistances (s.m^{-1}), Δ is the slope of the saturation vapour pressure temperature relationship (kPa.^{o}C^{-1}), γ is psychrometric constant (kPa.^{o}C^{-1}), c_p is the specific heat capacity of air at constant pressure (MJ.kg^{-1o}C^{-1}), ρ_a is the mean air density (kg.m^{-3}).

The soil water balance method and the crop coefficient method are the two empirical approaches used to estimate evapotranspiration. The crop evapotranspiration (ET$_c$) for a specific crop is determined by first calculating the reference evapotranspiration (ET$_o$) and then multiplying it by the crop coefficient (K$_c$), using Equation 2.7 (Irmak, 2009). There are a number of factors which influence K$_c$. This includes the crop type (which affects albedo, leaf properties, height, aerodynamics and stomata), the climate, crop growth stage and soil evaporation (Allen *et al.,* 1998). During the early growth stage K$_c$ is relativity low and increases toward the crop development stage until it reaches its maximum during mid-season after which it tends to decrease later on the growing season (Allen *et al.,* 1998). An example of the variation of K$_c$ is depicted in Figure 2.1.

$$ET_c = K_c \times ET_o \tag{2.7}$$
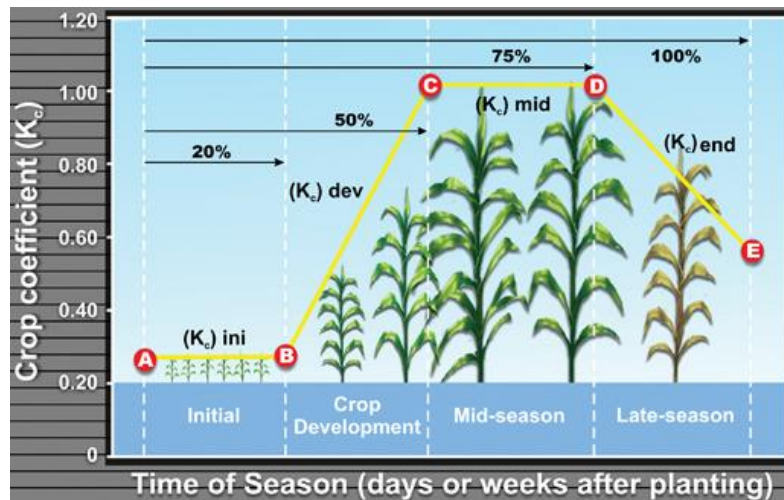
Figure 2.1   An example of crop coefficients (Irmak, 2009)

2.3   Remote Sensing of Total Evaporation

Remote sensing is described as the acquisition of data of the earth's surface without being in contact with it (Thoreson *et al.*, 2004). The basis for remote sensing is the electromagnetic spectrum, where the emitted or reflected radiation is measured (Engman, 1991). The spectral radiance of objects from the earth's surface is measured according to the electromagnetic spectrum (Engman, 1991). The sensors that are used to measure the spectral radiation are mounted on platforms. These platforms include ground-based, aircraft-based and satellite-based platforms (Engman, 1991). Thoreson *et al.* (2004) explains that for the case of evaporation estimates, satellite-based and aircraft-based platforms are generally used. There are four modelling approaches available to estimate ET which include: the empirical (direct) method, the residual of the energy balance method, the deterministic (indirect) method and the vegetation index method (Courault *et al.,* 2005). The SEBS model uses the residual of the energy balance approach. The residual of the energy balance method uses physical and empirical relationships to estimate ET (Courault *et al.*, 2005). Certain models derive input variables using remote sensing.

Some of the fundamental advantages of remote sensing, as highlighted by Li *et al.* (2009), are the ability to produce large spatial scale information, relatively cheap given that open-source software is used and images are freely available, and cover remote areas where humans cannot easily gain access to and install instruments. One of the disadvantages of remote

sensing is the amount of data required. The data required needs to be collected from a number of sources (Van der Tol and Parodi, 2011). The data is usually obtained from satellites or, in the case of meteorological data, from field measurements and is used as an input in the models (Van der Tol and Parodi, 2011). The satellite images require pre-processing such as atmospheric corrections, reflectance, radiance, and geo-referencing. Ground-based data is also required to validate the results obtained from remote sensing. Van der Tol and Parodi (2011) explain that the user can be faced with both scientific and practical difficultly during the data collection phase. The scientific problem faced by the user is the use of data obtained from various spatial and temporal scales (Van der Tol and Parodi, 2011). This requires the user to alter the data into the same spatial and temporal scale before using the data (Van der Tol and Parodi, 2011). The practical problems faced by the user include: data collection, the complexities involved using Geographic Information System (GIS), such as merging, and formulating the required algorithms to determine ET. The final ET result is dependent on the accuracy and reliability of the input data used (Van der Tol and Parodi, 2011). According to Van der Tol and Parodi (2011), there is an effort being made to produce a standard procedure for data merging, temporal and spatial alterations and to validate the processes that are used. The most common limitation is attaining cloud-free and high quality images (Jin *et al.*, 2013; Ma *et al.*, 2012). The revisit time of satellites vary from daily (MODIS) to every fortnight and in some cases longer (NASA, 2010). Landsat 7 and 8 has a revisit time of 16 days (NASA, 2010). This limits the user to a few images, depending on the study period. This reduces the number of images available to the users, which may impact the credibility of the study. On days that the satellite does pass it may be cloudy therefore, the next time a clear image could be captured is the next revisit which is 16 days later.

The widely used residual methods of the surface energy balance models that use remotely sensed surface temperature data to estimate spatial ET will be discussed in the following section.

2.3.1 Brief description of various remote sensing models using the residual of the energy balance method

A number of remote sensing based models that vary in complexity exist for estimating ET at large scales. However, only models applied in South Africa will be discussed here. Gibson *et al.* (2013) described a number of studies which use the residual of the energy balance approach to estimate ET in South Africa. The most common models used were the Surface

Energy Balance Algorithm for Land (SEBAL), Mapping Evapotranspiration with Internalised Calibration (METRIC), Surface Energy Balance System (SEBS) and Vegetation Index Surface Temperature Triangle/Trapezoidal model (VITT). The SEBAL model is the most applied model followed by SEBS, METRIC and VITT.

The SEBAL model was developed by Bastiaanssen *et al.* (1998). The SEBAL model uses surface reflectance, Normalized Difference Vegetation Index (NDVI) and surface temperature to determine surface fluxes (Bastiaanssen *et al.,* 1998). ET is determined by estimating R_n, G_o and H, using Equation 2.2, 2.4 and 2.5, respectively. One of the major disadvantages of the SEBAL model is the impact on the estimation of ET during advective conditions. A study by Mkhwanazi and Chavez (2013) illustrated the sensitivity of the model to advection due to evaporative fraction being fixed for the entire day. The evaporative fraction (EF) determined at the time the satellite overpass is assumed to be the same throughout the day and then used to estimate ET for the entire day (Mkhwanazi and Chavez, 2013). Mkhwanazi and Chavez (2013) reported errors of up to 45 % when compared to *in-situ* measurements (Lysimeter) over alfalfa crops in Colorado. When warm and windy conditions were present, the largest errors were recorded. Another study by Singh *et al.* (2008; cited by Mkhwanazi and Chavez, 2013) confirmed the impact of advection on ET. On average SEBAL produced results within 5 % of *in-situ* measured ET however, during advective conditions the results were recorded to be within 28 % of the *in-situ* ET measurements.

The advantages of SEBAL include:

- The model does not require large amounts of ground-based data (Li *et al.,* 2009; Mkhwanazi and Chavez, 2013; Liou and Kar, 2014).
- The presence of an automatic calibration within the model reduces the need for surface temperature correction relating to atmospheric effects (Li *et al.,* 2009; Liou and Kar, 2014).
- The internal calibration is possible for each image analysed (Li *et al.,* 2009; Liou and Kar, 2014).

The disadvantages include:

- When the model is applied over heterogeneous terrain, adjustments need to be made to account for the lapse rate, hence the model has been applied in most cases, over flat surfaces due to this (Li *et al.,* 2009).

- H is very sensitive to surface and air temperatures. An error in these temperatures will result in inaccurate estimates of H (Li *et al.,* 2009; Liou and Kar, 2014).

- Radiometer viewing angles effects have not been taken into account, which has a large influence on T_s (Li *et al.,* 2009).

- One disadvantage of the model is the possibility of ET to be underestimated during advection (Mkhwanazi and Chavez, 2013).

- The model code or pre-packaged version are not freely available.

- The need to define hot and cold pixels introduces subjectivity in the model outputs.

The SEBAL model has been applied in a study to estimate ET from Invasive Alien Plants (IAPs), indigenous vegetation and exotic forest plantations in the Western Cape and KwaZulu-Natal provinces (Meijninger and Jarmain, 2014). The model produced ET estimates using MODIS satellite images, however, a comparison between the SEBAL ET and *in-situ* ET data was not possible. Arising from its application to estimate biomass water use efficiency, biomass production and ET, the SEBS model was used for operational purposes to provide data at a weekly time-step for various agricultural crops (Gibson *et al*., 2013). GrapeLook was a website designed to provide remote sensing data, obtained using the SEBAL model, for table and wine grapes. This work was extended to sugarcane and grain crops with the studies being carried out by Jarmain and Klaasse (2012), and became known as FruitLook. Jarmain *et al.* (2009b) applied the model at a number of sites (*viz.* Seven Oaks, Midmar, St. Lucia and Kirkwood) to estimate ET.

The METRIC model was developed by Allen *et al.* (2007) and is a variant of the SEBAL model (Allen *et al.,* 2007). The METRIC model is based on the same assumptions as SEBAL for the hot pixel however, for the cold pixel a well vegetated surface (alfalfa reference ET) is used and is therefore partly calibrated with ground-based alfalfa reference ET. METRIC also differs from SEBAL in the way the daily ET is estimated from instantaneous ET calculated at the time of the satellite overpass. The evaporative fraction (EF) is assumed to be the same at both the observation time and for the 24-h period for SEBAL. In METRIC, the fraction of reference ET (ET_rF) is used to extrapolate the observation time to the 24-h period, instead of EF. ET_rF is the same as crop coefficient (K_c) and is defined as the ratio of ET to ET_r (alfalfa

reference) (Allen *et al*., 2007). The main inputs of the model are *in-situ* meteorological data, a digital elevation model (DEM) and long and short wave thermal images, such as MODIS and Landsat (Allen *et al.,* 2007).The METRIC model was developed to produce high resolution ET maps at scales less than a few 100 km (Allen *et al.,* 2007). The model was designed to account for advection and produce much more accurate estimates of ET than other models (Allen *et al.,* 2007). However, with that comes the need of meteorological data at a time step of an hour or less, a trained specialist with sound knowledge in radiation physics, energy balance and vegetation characteristics (Allen *et al.,* 2007).

The advantages of METRIC over other remote sensing energy balance models is that:

- Calibrated, using ET_o instead of evaporative fraction.

The advantages it has over traditional ET methods:

- ET can be determined for periods during water shortages.
- The crop type nor growth stage needs to be known.

The disadvantages of the METRIC model:

- Requires a highly specialized person to operate the model (Allen *et al.,* 2007).
- The selection of hot and cold pixels are dependent on the user's ability (Allen *et al.,* 2007).

The various components of the energy balance are determined based on Equations 2.3, 2.4 and 2.5. R_n is derived from surface temperature and the narrow-band reflectance, G_o is determined from the vegetation indices and the range in surface temperatures and H is determined from wind speed, surface roughness and ranges in surface temperature (Allen *et al.,* 2007). The METRIC model was applied by Jarmain *et al.* (2009b) to estimate ET at Seven Oaks. Only one image was used and the modelled ET using METRIC was recorded to be lower than the *in-situ* ET (Large Aperture Scintillometer) for September.

The vegetation index/temperature (VIT) trapezoid was proposed by Moran *et al.* (1994) to assist the crop water stress index (CWSI) by incorporating surface temperature and vegetation indices (Moran *et al.,* 1994). This method allowed the development of a new

approach, which estimated ET of fully and partially covered vegetation (Moran *et al.,* 1994). The main *in-situ* measurements required for the VIT trapezoid are air temperature, stomatal resistance (maximum and minimum), wind speed and vapour pressure (Li *et al.,* 2009). An assumption to the model is that a trapezoidal shape will form if T_s (surface temperature)-T_a (air temperature) is plotted against vegetation cover (Jarmain *et al.,* 2009b). The edges of the trapezoid refer to four different conditions, such as (a) a bare soil, (b) saturated bare soil, (c) water stressed vegetation, soil fully covered and (d) well-watered vegetation, soil fully covered (Jarmain *et al.,* 2009b; Li *et al.,* 2009).

Daily ET is dependent on potential ET (PET) and the soil moisture availability index (M_a), which is described in Equation 2.8, and is determined from instantaneous evaporation (Jarmain, *et al.,* 2009b).

$$Ma = 1 - WDI = \frac{LE}{LE_p} = \frac{[(T_s - T_a)_{min} - (T_s - T_a)_i]}{[(T_s - T_a)_{min} - (T_s - T_a)_{max}]} \qquad (2.8)$$

where, WDI is water deficit index, λE is latent energy flux (W.m^{-2}), LE_p is potential ET (W.m^{-2}), $(T_s\text{-}T_a)_{max}$ and $(T_s\text{-}T_a)_{min}$ is the difference between the maximum and minimum surface and air temperature (K).

The advantage of the VIT trapezoidal model is that it does not require a large amount of pixels like the VIT triangular method. However, it requires more ground-based parameters than the VIT triangular method (Li *et al.,* 2009). Although the WDI is a promising method it has a number of limitations. Li *et al.* (2009) state that heat exchanges between the soil and vegetation are not accounted for, the transpiration and soil evaporation components are not separated and vegetation cover is not instantaneously effected by water stress.

Jarmain *et al.* (2009b) applied the model at three sites to estimate ET. The first site, Seven Oaks, consisted of *Acacia mearnsii*. The St. Lucia site consisted of swamp forest, burnt grasslands and sedges wetland and the Kirkwood site had degraded land and spekboom veld. The VITT model produced significantly lower ET estimates for the *Acacia mearnsii* vegetation compared to the over-estimation of ET for the spekboom veld relative to the *in-situ* ET. For the forest and sedges vegetation the modelled ET results were not consistent (45 % difference) with the *in-situ* ET data. However, for the grasslands and degraded site the model produced a favourable comparison to the *in-situ* ET. The *in-situ* ET was measured using an eddy covariance and surface renewal for the forest, a large aperture scintillometer

for the sedges vegetation and a surface renewal and scintillometer for the grasslands (Jarmain *et al.,* 2009b).

The SEBS model was developed by Su (2002) and is a free, open-source model available in ILWIS. The model was developed to be used in conjunction with satellite imagery to determine turbulent fluxes in the atmosphere. The model requires meteorological data at various scales, depending on the scale of study (Su, 2002). It is highlighted by Su (2002) that the model utilises spectral reflectance and radiation to determine various land surface parameters, including vegetation cover, emissivity, temperature and albedo. The ability to determine roughness length required to obtain heat transfer and the evaporative fraction is also possible (Su, 2002). The model has been applied a number of times in South Africa. Jarmain *et al*. (2009b) investigated ET from the Seven Oaks, St. Lucia and Kirkwood sites. At the Seven Oaks and St. Lucia sites the model performed fairly well compared to the Kirkwood site where the model was unable to produce a reliable estimate of ET. Gibson *et al.* (2011) applied the model in the Piketberg region to determine the uncertainties regarding the model, Mengistu *et al.* (2014) used the model to estimate ET at field-scale at Baynesfield and most recently Shoko *et al.* (2015b) estimated ET over a heterogeneous catchment in KwaZulu-Natal. These studies are discussed in the next section.

The advantages of the SEBS model include:

- Open-source model available in ILWIS.
- Physical parameterizations used to solve the energy balance in SEBS.
- Fewer assumptions than other techniques.

The disadvantages of the SEBS model include:

- Evaporative fraction assumed to be constant.
- Method to determine turbulent heat flux is complex.
- A number of parameters are required.

All the aforementioned models were taken into consideration for this study. Following the evaluation of the advantages and disadvantages of each, the SEBS model was chosen for this study based on its wide application in South Africa and it could be easily obtained as it was a free, open-source model. The model is explained in detail in the next sub-section.

2.4 The Surface Energy Balance System (SEBS) Model

The SEBS model requires three sets of input information *viz.* vegetation data, climatic data and spectral radiation information (Su, 2002). The vegetation information required by the model include the fractional vegetation cover, vegetation height, leaf area index. Land surface albedo, surface emissivity and surface temperature are also required. Su (2002) explained that, when vegetation information is restricted, the Normalised Difference Vegetation Index (NDVI) can be used.

The climatic components that are required consist of wind speed (at reference height of 1.8m), relative humidity, air temperature and air pressure. This information can be obtained from meteorological models or an automatic weather station (Su, 2002). The final set of information required is the downward solar radiation and longwave radiation, which can be obtained from a number of sources, such as field measurements, models or parameters (Su, 2002).

The SEBS model utilises the energy balance equation, Equation 2.1, to estimate daily evapotranspiration (Su, 2002). Su (2002) describes the various steps, in detail, which derive the final equation to estimate daily actual ET. The net radiation component is explained in Equation 2.9.

$$Rn = (1-\propto)R_{swd} + \varepsilon R_{lwd} - \varepsilon \sigma T^4 \qquad (2.9)$$

Where, R_{lwd} is longwave radiation (W.m^{-2}), R_{swd} is shortwave solar radiation (W.m^{-2}), surface emissivity is denoted by ε and the Stefan-Boltzmann constant is represented by σ. Surface temperature is represented by T (K) and surface albedo is $\propto$ (Su, 2002).

The soil heat flux (G_o) component, Equation 2.10, consists of Γ_c and Γ_s, which represent values for different land covers representing the ratio of soil heat flux to net radiation (Su, 2002). Full vegetation cover is represented by Γ_c, which is equal to 0.05, whereas bare soils (Γ_s) is equivalent to 0.315 (Su, 2002). These are known as the limiting cases. The fractional canopy coverage (fc) is then interpolated between Γ_c and Γ_s (Su, 2002).

$$Go = Rn(\Gamma c + (1 - fc)(\Gamma s - \Gamma c)) \qquad (2.10)$$

The Normalized Difference Vegetation Index (NDVI) is used in the interpolation of fc as demonstrated in Equation 2.11. Full vegetation cover is represented by $NDVI_{max}$, where $fc=1$ and $NDVI_{min}$ represents bare soil with $fc=0$ (Jin, 2013).

$$fc = \frac{NDVI - NDVImin}{NDVImax - NDVImin} \qquad (2.11)$$

The limiting cases are used to calculate the evaporative fraction (Su, 2002). The wet and dry limits are determined, as illustrated in Equations 2.12 and 2.13. The latent heat, under the dry-limit is equal to 0 as a result of soil moisture limitation, whereas the maximum value is allocated to the sensible heat flux (Su, 2002). The sensible heat flux value is given a minimum value under the wet-limit and the energy given off the surface and atmospheric conditions is used to obtain ET (Jin *et al*., 2013).

$$Hdry = Rn - Go \qquad (2.12)$$

$$Hwet = Rn - Go - LEwet \qquad (2.13)$$

The relative evaporation (Equation 2.15) is obtained based on the H_{dry} and H_{wet} equations above.

$$(2.14)$$

$$\wedge r = 1 - \frac{H - Hwet}{Hdry - Hwet}$$

The next step in the SEBS algorithm involves determining the evaporative fraction using Equation 2.15. This is obtained by substituting Equations 2.9, 2.12 and 2.13 with Equation 2.15. The evaporative fraction describes the energy required for the evapotranspiration process (Jin *et al*., 2013).

$$\wedge = \frac{LE}{H+LE} = \frac{LE}{Rn-Go} = \frac{\wedge rLEwet}{Rn-Go} \qquad (2.15)$$

In order to determine the actual daily evaporation (E_{daily}), it is assumed that the evaporative fraction is equal to the instantaneous value (Su, 2002). E_{daily} is evaluated using Equation 2.16.

$$E_{daily} = 8.64 \times 10^7 \times \frac{\wedge R_n}{L\rho_w} \qquad (2.16)$$

where, E_{daily} is the actual daily evaporation (mm.day^{-1}), R_n is the daily net radiation (W.m^{-2}), ρ_w is the density of water (kg.m^{-3}) and L is the latent heat of vaporization (J.kg^{-1}).

Su (2002) conducted an experiment on three vegetation types (cotton, shrubs and grass) to assess its reliability. Given that the geometrical and physical variables are reliable, it was deduced from the study that:

- SEBS mean error is 20% relative to measured H.

- SEBS is able to provide reliable estimate of H at local and regional scales.

There are however, some factors to take into consideration. An appropriate formula should be selected for the fractional vegetation cover and where possible a leaf area index (LAI) product may be used. SEBS should not be applied in mountainous areas with coarse resolution data as inaccurate estimates of surface temperature is expected due to the heterogeneity of the area. The height of the weather station in relation to the vegetation under study should be considered. Vegetation exceeding a height of 2.7 m should obtain wind speed measurements from stations at 10 m (Gibson *et al.*, 2011).

Su (2002) explains that the SEBS model is capable of producing acceptable estimates of turbulent heat flux at various spatial scales. This is supported by local and international studies. Mengistu *et al.* (2014) conducted a field scale study to estimate satellite based ET and soil moisture for the calibration of hydrometeorological models. The study was carried out in the Baynesfield Estate in KwaZulu-Natal, South Africa. The SEBS model overestimated ET by 15%. A regional scale study by Ma *et al*. (2014) was conducted in Namco, China. The Advanced Space-borne Thermal Emission and Reflection Radiometer (ASTER) satellite data was used as input to SEBS to estimate ET for 11 June 2006 and 25 February 2008. The SEBS ET estimates were 30-40% higher than the ground-based ET measurements, however, an RMSE of 0.7 mm.day^{-1} was achieved and the seasonal variation was well captured using the SEBS model.

Gibson *et al.* (2011) explains that there is uncertainty related to the heterogeneity of the study area, the choice of fractional vegetation cover equation, the surface and air temperature gradient and the height of wind speed in relation to displacement height. However, the uncertainties can be reduced by selecting a sensor that will capture the heterogeneity of the land. For local scale a high resolution sensor (Landsat) should be used whereas coarse resolution sensors (MODIS) are appropriate at regional scale (Gibson *et al.,* 2011). Shoko *et al.* (2015b) estimated ET in the uMngeni catchment in South Africa. The study focused on

applying two multi-spectral sensors, namely Landsat 8 and MODIS, to assess the influence of spatial resolution. Landsat 8 has a 30m spatial resolution, whereas MODIS has a 1000m spatial resolution. The uMngeni catchment is a heterogenous catchment that consists of subsistence and commercial agriculture, urban areas, indigenous and commercial forestry. The results from the study indicated that the Landsat 8 sensor was able to provide a more accurate representation of the various land uses and followed the trend of the *in-situ* ET measurements more closely than the MODIS senor data. It was recommended by Shoko *et al.* (2015b) that the MODIS sensor would be ideal for a large homogenous catchment. The use of the MODIS sensor proved applicable for a study over the Tibet Autonomous Region by Zhuo *et al.* (2014). The MODIS satellite was able to cover the large catchment and provide estimates of ET. Although the SEBS ET estimates did overestimate and underestimate in some cases, the general trend was consistent with the *in-situ* measurements.

One of the points raised by Gibson *et al.* (2013) was that the SEBS model should be restricted to agricultural areas. There has, however, been a number of studies outside this area of recommendation which indicate the models ability to provide reliable estimates of ET over various land uses. Singh and Senay (2016) conducted a study in Midwestern, United States using different energy balance models, namely, the METRIC, SEBAL, SEBS and the Operational Simplified Surface Energy Balance (SSEBop) model. For the study four Landsat 5 TM and four 7 ETM+ images was used. The sites consist of centre-pivot maize, soybean, rainfed maize-soybean and the surrounding urban areas. The various models were used to capture the temporal and spatial variation in and around the study site, including urban areas. The results from the study indicate that the SEBS ET from urban areas was consistent throughout. Elhag *et al.* (2011) applied the SEBS model to estimate ET and evaporative fraction for the Nile Delta, Egypt. The study focused on the agricultural fields, however, the area is a heterogeneous region with land uses such as fish farms and urban areas. Using *in-situ* ET data from around the study area a R^2 value of 0.84 was achieved. Huang *et al.* (2015) conducted a study in a desert-oasis located in the Heihe River Basin, China. The study investigated the influence of soil moisture on ET using MODIS imagery. The study area consisted of various land covers including wheat, maize, Gobi desert, desert steppe and sandy desert. *In-situ* ET data was collected from various sites such as, maize, vegetable, villages and orchards. An overall RMSE of 84.1 ($W.m^{-2}$) was achieved for sensible heat flux. Tian *et al.* (2015) applied the SEBS model to forest in the Qilian Mountains. *In-situ* ET measurements were recorded for a two year period using an eddy covariance system. The

comparison of SEBS ET to *in-situ* ET resulted in a R^2 value of 0.8. SEBS was slightly lower during the summer and autumn months for 2010 but higher ET estimates was estimated for the same seasons in 2011.

2.5 Discussion

The assessment against the baseline gives an estimate of the impact of land use on the hydrological responses. This can help aid decisions for water resources management and planning as well as, for example, the issuing of licences relating to afforestation (DWAF, 1999). The SANBI (2012) land cover map provides greater detail of natural vegetation compared to, the currently accepted, Acocks' (1988) Veld Types but lacks water use information. There are a number of methods available to estimate ET. The conventional ground-based measurement methods were described in this Chapter. However, these methods estimate ET based on point or line averaged measurements, which are only representative of local scales and cannot be extended to large areas because of land surface heterogeneity (French *et al*., 2005). Remote sensing has the ability to overcome this and produce large spatial scale estimates of ET (Gibson *et al.,* 2013). It can also provide information at remote sites where it is difficult to install instruments (Wagner *et al.,* 2009). However, ET cannot be directly estimated using satellite remote sensing (Wagner *et al.,* 2009). Remote sensing data needs to be combined with models that quantify the interaction of water and energy arising from the land surface and atmosphere (Wagner *et al.,* 2009). Four remote sensing models based on residual of the energy balance were investigated *viz.* SEBAL, SEBS, METRIC and VITT. The VITT and METRIC models were limited in their application in South Africa. The SEBAL model was applied extensively in South Africa. However, it was protected by intellectual property and was not freely available to use. The SEBS model was widely applied locally and internationally and is freely available for research purposes. There have been a number of studies that applied SEBS over agricultural fields. However, recent literature indicate the models potential to estimate ET over natural vegetation with a degree of confidence. The following Chapter describes the methodology used to estimate ET across seven biomes in South Africa using the SEBS model.

3. METHODOLOGY

Measurements of ET help provide information of water use from vegetation. Large scale estimates of ET using *in-situ* methods are not possible. However, the advent of remote sensing can help minimise this limitation due to the large spatial scale that the image covers. This chapter explains the method used to estimate ET over natural vegetation in South Africa. The SEBS model in conjunction with Landsat satellite imagery was used to provide point-based and large scale spatial estimates of ET for the different biomes across the country.

The methodology is separated into two categories in order to address the first two research questions as outlined in Chapter 1. The research questions are:

i. How do the SEBS estimates of ET for natural vegetation compare to *in-situ* ET measurements over natural vegetation?

ii. How does ET vary (seasonally and spatially) between the various South African biomes?

To address the first research question the SEBS model was set up to estimate ET for various sites within South Africa where *in-situ* ET estimates over natural vegetation were available. A comparison of *in-situ* ET and remote sensing ET was undertaken to investigate the accuracy of remotely sensed ET of natural vegetation. This was used for validation to determine the reliability of remotely sensed ET estimates.

Following the validation of the SEBS ET estimates, the SEBS model was applied to estimate ET for seven biomes in South Africa to address the second research question. These include the Grasslands, Fynbos, Forest, Albany Thicket, Indian Ocean Coastal Belt, Nama Karoo and Savanna biomes. The Azonal Vegetation, Succulent Karoo and Desert Biomes were omitted due to the lack of measured ET. The period between 1 July 2014 and 31 June 2015 was selected to estimate ET, as a long term record of ET is required to identify seasonal variation.

3.1 Description of Study Sites

Based on the availability of measured ET for natural vegetation, one research site per biome (Figure 3.1) was identified. Seven sites were identified as *in-situ* ET data could not be attained for the Azonal Vegetation, Succulent Karoo and Desert biomes. A biome is

described as "a high-level hierarchical unit having a similar vegetation structure exposed to similar macroclimate patterns, often linked to characteristic levels of disturbance such as grazing and fire" (Mucina and Rutherford, 2006: 32). The main climatic factors that influence the survival and establishment of plants within the biome are temperature and soil moisture (SANBI, 2016). Each of the sites selected are described below.
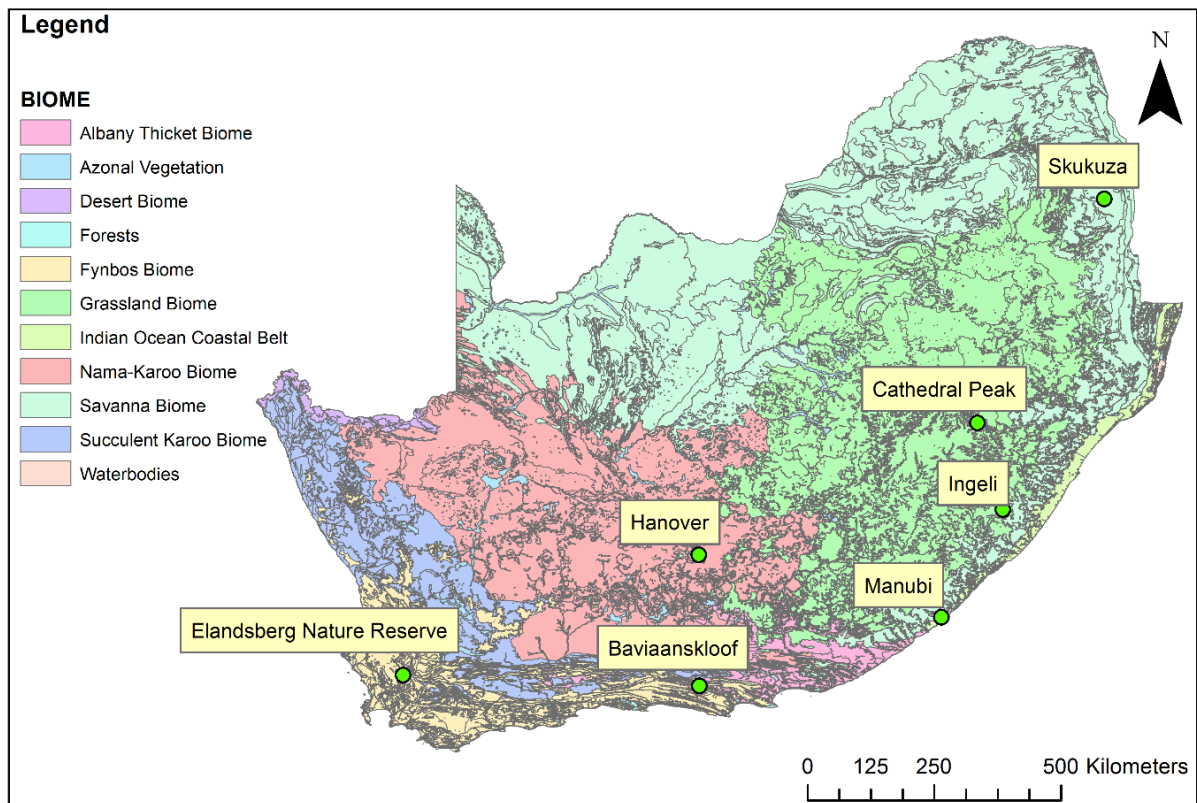
Figure 3.1   Map illustrating the South African vegetation biomes (SANBI, 2012) and the sites selected for the study where *in-situ* ET and meteorological data could be obtained

The Cathedral Peak Research catchments (28° 59' 59" S, 29° 14' 59" E), situated in the mountainous region of the KwaZulu-Natal Province, were used to represent the grasslands biome. The research catchments experience summer rainfall with a mean annual precipitation (MAP) of 1400 mm.y^{-1} (Warburton, 2014). The altitude of the catchment ranges from 1820 m to 2463 m (Warburton, 2014). The Cathedral Peak catchments were selected to represent the Grassland biome as ET and meteorological data was monitored by SAEON GWF node, Dr. Mengistu and colleagues for the period 12 July 2014 to 30 July 2015 using an eddy

covariance system and automatic weather station (AWS). According to SANBI (2012) the monitoring site lies in the uKhahlamba Basalt Grasslands, making it an ideal site to represent the Grassland biome.

The Elandesberg Nature Reserve (ENR) (19° 03' 25" S, $33^o28'10$" E) was selected to represent the Fynbos biome. The ENR is located at the foot slope of the Elandskloof mountain in the Western Cape Province at an elevation of 150 m (Dzikiti *et al.,* 2014). The area experiences winter rainfall with a MAP of 470 mm.y^{-1}. Temperatures in the region reach 43^oC in summer and drop to as low as 2^oC in winter (Dzikiti *et al.,* 2014). ET and meteorological data was monitored by Dzikiti *et al.* (2014) from 1 November 2012 to 31 October 2013 using a boundary layer scintillometer and an AWS. According to SANBI (2012) and Dzikiti *et al.* (2014) the study site lies within the Swartland Alluvium Fynbos.

The Ingeli State Forest (30° 31' 48" S, 29° 42' 0.14" E) falls within the Forest biome as described by SANBI (2012). The site is in the southern region of KwaZulu-Natal at an elevation of 1232 m (Gush and Dye, 2015). The area experiences a MAP of between 804 to 1123 mm.y^{-1} with most of the precipitation occurring in the form of mist during summer (Gush and Dye, 2015). ET and meteorological data, using an eddy covariance and AWS, was measured by Gush and Dye (2015) for a week in October 2011 and May 2012. A longer set of ET measurements were conducted from 5 December 2012 to 11 February 2013.

The Manubi forest (32° 26' 59" S, 28° 35' 24" E) found in the Eastern Cape Province was selected to represent the Indian Ocean Coastal Belt biome (SANBI, 2012). According to SANBI (2012) and Gush and Dye (2015) the forest is described as Transkei Coastal belt. The Manubi forest is situated at a maximum elevation of 230 m and has a MAP of 1070 mm.y^{-1} (Gush and Dye, 2015). ET and meteorological measurements, using an eddy covariance system and an AWS, were conducted by Gush and Dye (2015) for window periods from 3 September 2010 to 7 September 2010, 24 February 2011 to 2 March 2011 and 11 May 2011 to 18 May 2011.

The study site selected in the Nama Karoo biome in the Northern Cape Province was used in a study by Everson *et al.* (2009) where the evaporation from dryland karoo shrubland located along the upper reach of the Seekoei River was investigated using a scintillometer. The site (31° 19' 59" S, 24° 17' 59" E) is 20 km south west from Hanover on Vanzylskraal farm (Everson *et al*., 2009). The data was recorded between the 6 January 2008 and 14 January

2008. The area falls within the summer rainfall region and has a MAP between 300 to 420 mm (Everson *et al*., 2009).

The Baviaanskloof study site (33° 39' 0.014" S, 24^o19' 0.018" E) was selected to represent the Albany Thicket biome. The Baviaanskloof is located in the Eastern Cape Province. Summer maximum temperatures can reach over 40^oC with winter minimums around 0^oC (Baviaans Tourism, 2012). The evenings experience cool conditions as a result of the easterly sea winds (Baviaans Tourism, 2012). The area receives a MAP of approximately 200 mm.y^{-1} (Knight, 2012). SANBI (2012) describe the vegetation type in this area as Groot Thicket. A study by Dr. Mengistu and colleagues measured ET rates at the site from 16 September 2008 to 7 October 2008 using an eddy covariance system.

The Skukuza flux tower (23° 01' 11" S, 31° 29' 48" E), located in the North-eastern region of South Africa, falls within the Savanna biome (Ramoelo *et al.,*2014) and was thus selected to represent this biome. The area where the flux tower is stationed experiences a MAP of 547 mm.y^{-1} with the majority of the rainfall falling in the summer season (Ramoelo *et al.,* 2014). The vegetation type is described as granite lowveld (SANBI, 2012). ET data from 26 July 2013 to 26 May 2014 was used in this study.

3.2   SEBS ET Data Acquisition and Processing

3.2.1   Satellite and meteorological data acquisition

The ET and meteorological data was sourced from the respective researchers who conducted the measurements at the selected sites. The ET data was measured using conventional techniques which include the scintillometer and eddy covariance system. Automatic weather stations were used to measure solar radiation, wind speed, air temperature, relative humidity and air pressure (Everson *et al.,* 2009; Dzikiti *et al.,* 2014; Gush and Dye, 2015). The measurement period, number of images obtained and the source from which the data was obtained for each biome is provided in Table 3.1. Due to the various time periods that the ET data was measured, both Landsat 7 and 8 satellite imagery were required as each satellite covered a different historical period. The satellite used for each site is shown in Table 3.1. The Landsat 7 ETM+ and Landsat 8 OLI/TIRS images used for this study were accessed from the United States Geological Survey site (http://landsat.usgs.gov). Landsat 7 and 8 satellites are in orbit and follow the Worldwide Reference System (WRS-2) (USGS, 2015). Landsat 7 and 8 satellites have been operational since April 1999 and February 2013,

respectively (USGS, 2015). The satellites have a temporal resolution of 16-days and a spatial resolution of 30 m. The number of images obtained was restricted due to the availability of cloud free images and the temporal resolution of Landsat. The site coordinates, study period and cloud-cover percentage was required to retrieve the images. For this study, images with a cloud cover of less than 10% were selected. The Level 1 GeoTIFF images were downloaded and processed in SEBS to estimate daily ET. The pre-processing of the images is described in the section which follows.

Table 3.1   Details of the study sites and data obtained

Biome	Site	Measurement period	Measurement method	Source	Landsat Satellite	No. of images
Grasslands	Cathedral Peak	01/01/14–31/05/15	Eddy covariance	Dr. Mengistu	8	8
Nama-Karoo	Hanover	06/02/08-14/02/08	Scintillometer	Everson *et al.* (2009)	7	1
Albany Thicket	Baviaanskloof	16/09/08-07/10/08	Eddy covariance	Dr. Mengistu	7	1
Indian Ocean Coastal Belt	Manubi	03/09/10-18/05/11	Eddy covariance	Gush & Dye (2015)	7	3
Fynbos	Elandsberg Nature Reserve	01/11/12-31/10/13	Boundary layer scintillometer	Dzikiti *et al.* (2014)	7	11
Forest	Ingeli	06/10/11-11/02/13	Eddy covariance	Gush & Dye (2015)	7	5
Savanna	Skukuza	2010-2014	Eddy covariance	(Ramoelo *et al.* 2014)	8	10

3.2.2   Pre-processing of Landsat images

Once the Level 1 image products were downloaded the bands were imported into the ILWIS 3.8 academic software (http://52north.org/communities/ilwis/ilwis-open/download). The GDAL tool was used to import the images and convert each band into digital numbers (DN). Once this was complete the image bands (in DN format) were ready for the pre-processing phase.

Landsat 7 ETM+ and Landsat 8 OLI/TIRS pre-processing differed slightly with regard to the equations used to convert the bands into radiance ($L\lambda$) and top of atmosphere (TOA) reflectance, the bands used to determine TOA albedo and the bands used to determine the Normalized Difference Vegetation Index (NDVI). The steps taken in the pre-processing phase are described in more detail in Figure 3.2.

Access http://landsat.usgs.gov and register/login and navigate to Earth Explorer

Input coordinates of study area and start and end date for study

Select Landsat 7 ETM+ SLC-off (2003-present) or Landsat 8 OLI/TIRS from Landsat Archive

Select cloud cover of <10% and day images

Download Level 1 Product images and unzip

Import into ILWIS 3.4 and convert the bands into Digital numbers (DN) using GDAL

Landsat 7 ETM+ SLC-off (2003-present)

Landsat 8 OLI/TIRS

Convert DN bands into radiance (Lλ) (NASA, 2010)

$$* L\lambda = \frac{Lmax - Lmin}{Qcalmax - Qcalmin} \times (Qcal - Qcalmin) + Lmin$$

Convert DN bands into radiance (Lλ) (NASA, 2015)

$$L\lambda = M_L Q_{cal} + A_L$$

TOA reflectance (ρλ) (NASA, 2010)

$$* \rho\lambda = \frac{\pi \times L\lambda \times d^2}{ESUN\lambda \times \cos\theta}$$

TOA reflectance (ρλ) (NASA, 2015)

$$* \rho\lambda' = M_p Q_{cal} + A_p$$

$$\rho\lambda = \frac{\rho\lambda'}{\sin(\theta_{SE})}$$

Figure 3.2   Flow chart displaying steps undertaken during pre-processing

Left column (NASA, 2010):

Convert band 6 into Brightness temperature (NASA, 2010)

$$T = \frac{K2}{\ln(\frac{K1}{L\lambda} + 1)}$$

Albedo

$$albedo = (albedo\_TOA - 0.03)/0.767\text{^}2$$

NDVI

$$NDVI = (ref\_4 - ref\_3)/(ref\_4 + ref\_3)$$

Fractional vegetation cover (FVC)

$$FVC = ((NDVI - NDVI\text{--}min)/(NDVI\text{--}max - NDVI\text{--}min))\text{^}2$$

Emissivity (Eo)

$$Eo = 0.004 * FVC + 0.986$$

Land surface temperature (LST)

$$LST = BT/(Eo\text{^}0.25)$$

Right column (NASA, 2015):

Convert band 6 into Brightness temperature (NASA, 2015)

$$T = \frac{K2}{\ln(\frac{K1}{L\lambda} + 1)}$$

Albedo

$$albedo = (albedo\_TOA - 0.03)/0.767\text{^}2$$

NDVI

$$NDVI = (C\_ref\_5 - C\_ref\_4)/(C\_ref\_5 + C\_ref\_4)$$

Fractional vegetation cover (FVC)

$$FVC = ((NDVI - NDVI\text{--}min)/(NDVI\text{--}max - NDVI\text{--}min))\text{^}2$$

Emissivity (Eo)

$$Eo = 1.009 + 0.047 * ln(NDVI)$$

Land surface temperature (LST)

$$LST = BT/(Eo\text{^}0.25)$$
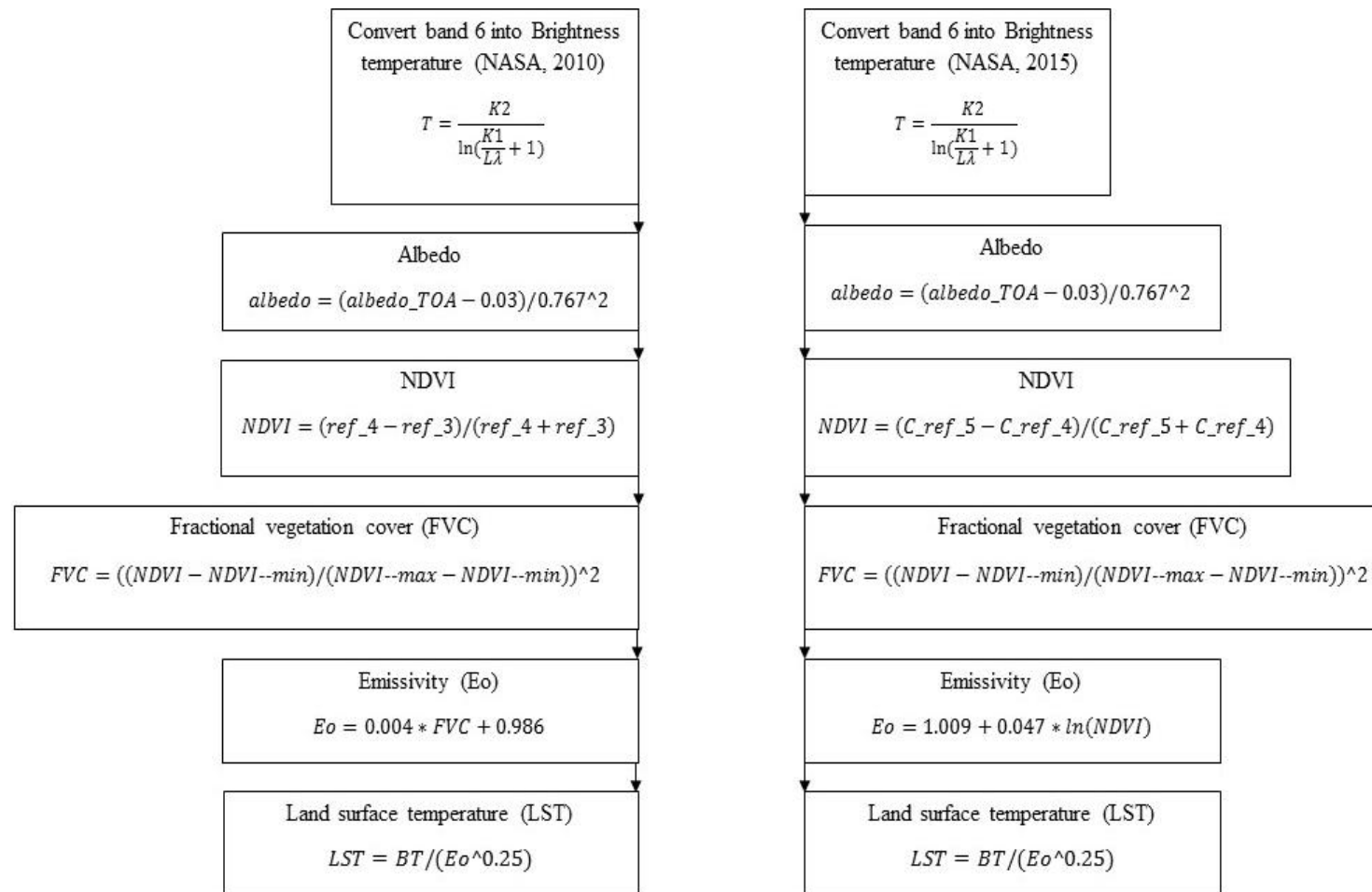
Figure 3.3 (Continued)   Flow chart displaying steps undertaken during pre-processing

3.2.3   SEBS processing

The aim of the pre-processing phase is to produce an albedo (α), NDVI, emissivity (ε_o), fractional vegetation cover and land surface temperature maps which are required in the final processing phase in the SEBS model. The aforementioned maps in conjunction with meteorological data, sun zenith angle, Digital Elevation Map (DEM), Julian day and sunshine duration was used as inputs in the SEBS Model to determine a number of outputs (Figure 3.3). The meteorological data used in the model include solar radiation (W.m^{-2}), windspeed (m.s^{-1}), mean daily air temperature (^{o}C) and air temperature (^{o}C) at satellite over pass time. This data was attained from the various research sites (Table 3.1). The DEM (90m) was obtained from Consortium for Spatial Information (CGIAR-CSI) (http://srtm.csi.cgiar.org/SELECTION/inputCoord.asp), the Julian day and sun azimuth angle (used to calculate zenith angle) were obtained from the metadata file of the image. An example of the inputs (albedo and NDVI) and outputs (Rn and λE) is shown in Figure 3.4.
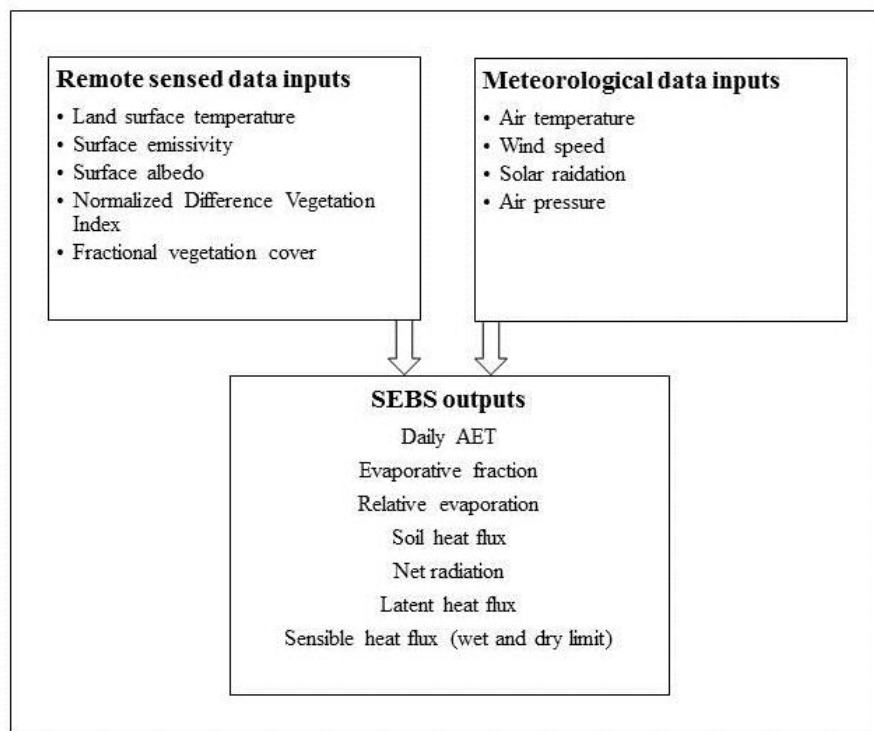

Figure 3.4   The   input   data   and   output   data   from   the   SEBS   model
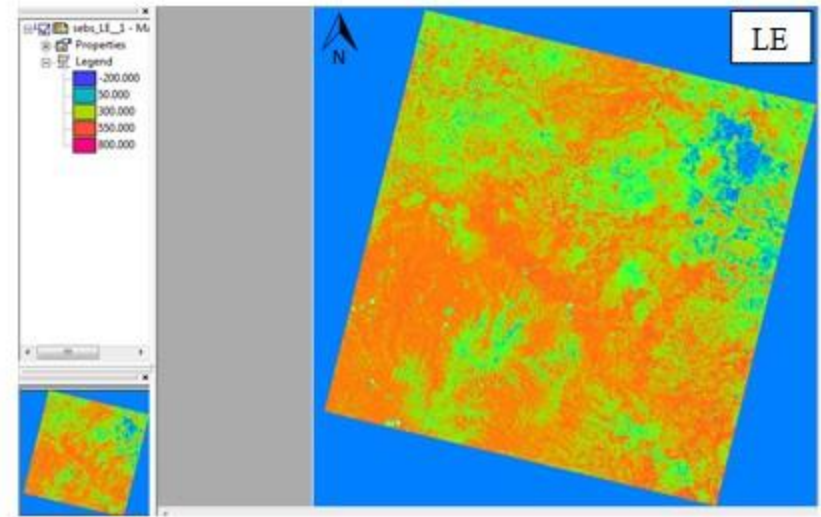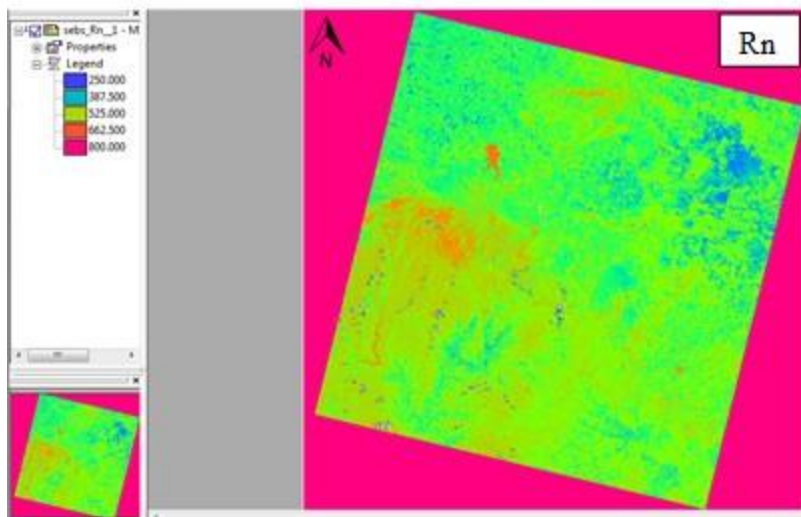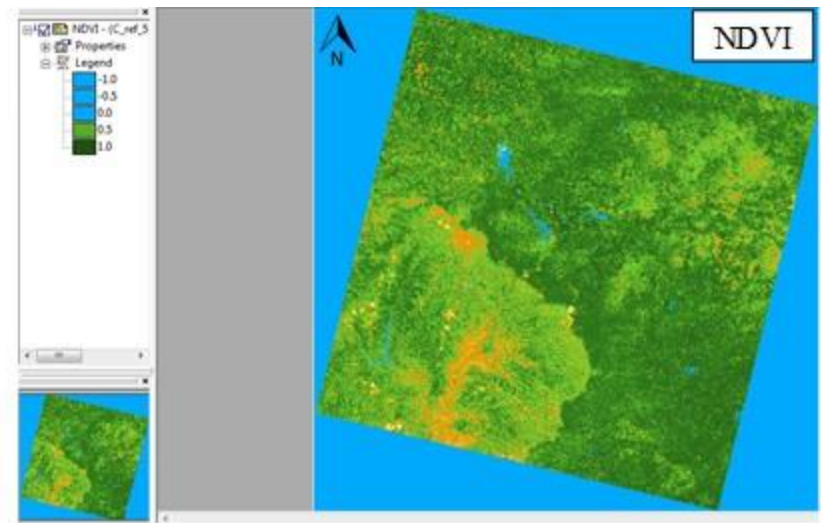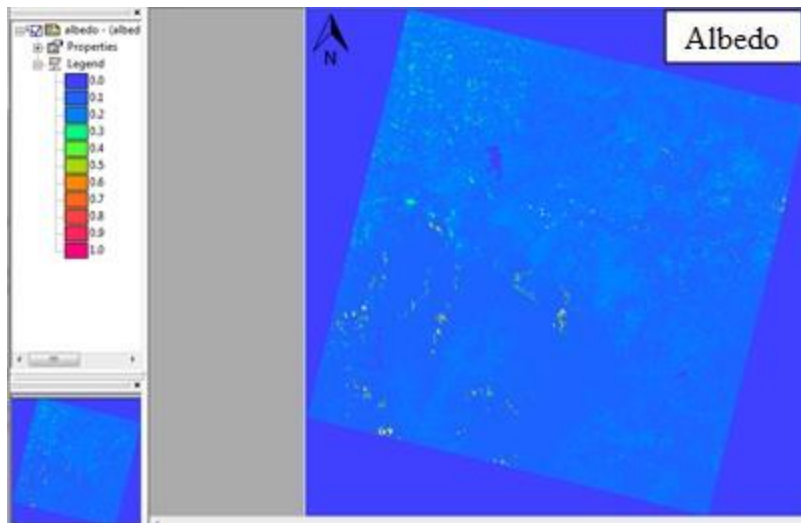
Figure 3.5   An example of SEBS remote sensing inputs (Albedo and NDVI) and outputs (Rn and λE) for the

Grasslands   biome   at   Cathedral   Peak   in   KwaZulu-Natal   on   12   January   2015

The SEBS model produces a number of output maps which include, evaporative fraction, relative evaporation, soil heat flux (G_o), net radiation (R_n), latent heat flux (λE), sensible heat flux (H) and daily evaporation. For this study only the daily evaporation map was required. The respective coordinates for each study site were used to identify the area and the pixel value at that location represented the daily ET estimation. The daily ET from SEBS was compared to the *in-situ* daily ET for each site. The SEBS ET and *in-situ* ET were plotted on a time series graph to analyse the trend and seasonal variation as well as the maximum and minimum ET. A regression graph was used to produce the R^2 value. The RMSE was also determined for each site. This process was applied for all the selected sites used in the study.

3.3   Modelling ET using SEBS

The second part of the study, aimed at addressing research question two, investigated the spatial and seasonal variation of daily ET between the biomes. As a year-long data set was required, cloud-free Landsat 8 OLI/TIRS images were downloaded for 1 July 2014 to 31 June 2015 for each biome.

3.3.1   Data collection

The satellite data acquisition and pre-processing of the images was conducted in the same manner as explained in Section 3.2.2 and illustrated for Landsat 8 in Figure 3.2. ArcGIS was used to clip each biome to ensure only the biome under investigation was present in the satellite image scene. One image was used for each biome. The entire image scene was used in this investigation to gain a larger spatial estimate of ET for each biome. This required a larger spatial representation of the meteorological parameters. The meteorological data (air temperature, mean air temperature and wind speed) was obtained from the South African Weather Service (SAWS). SAWS data was chosen due to the availability of long records and that data is available to students free of charge. No solar radiation data was available from the SAWS, therefore a model was used to compute hourly solar radiation. Solar radiation is the main driver for ET (Allen *et al.,* 1998). There are a number of models available to estimate daily solar radiation, however, the SEBS model requires solar radiation at satellite overpass time. The hourly solar radiation model by Allen *et al.* (1998) was selected as the variables required were easily attainable. The model was used to produce hourly solar radiation at each of the SAWS station sites for all the biomes.

Solar radiation (R_s) was determined using Equation 3.1, defined as:

$$Rs = (as + bs \times \frac{n}{N}) \times Ra \qquad (3.1)$$

where a_s and b_s are 0.25 and 0.5, respectively, n is the duration of sunshine (hours), N is the maximum duration of sunshine (hours) (n=N on clear days) and R_a is the extraterrestrial radiation (MJ.m.$^{-2}$day^{-1}).

Since cloud free images were selected for this study, the relative sunshine duration (n/N) was equal to 1. The extraterrestrial radiation (R_a) was given by:

$$Ra = \frac{12(60)}{\pi}. Gsc. dr[(\omega_2 - \omega_1)\sin(\varphi).\sin(\delta) + \cos(\varphi).\cos(\delta).(\sin(\omega_2) - \sin(\omega_1))] \qquad (3.2)$$

where, G_{sc} is a solar constant of 0.0820 MJ.m^{-2}.min^{-1}, dr is the inverse relative Earth-Sun distance (radians), ω_1 and ω_2 are the solar time angle at the beginning and end of the period (radians), respectively, φ is the latitude of the site (radians) and δ is the solar declination (radians)

The inverse relative Earth-Sun distance (dr) was determined using Equation 3.3:

$$dr = 1 + 0.033\cos(\frac{2\pi}{365} \times J) \qquad (3.3)$$

where, J is the Julian day.

ω_1 and ω_2 is given by Equation 3.4 and 3.5 as:

$$\omega_1 = \omega - \frac{\pi t_1}{24} \qquad (3.4)$$

$$\omega_2 = \omega + \frac{\pi t_1}{24} \qquad (3.5)$$

where, ω is the solar time angle at midpoint of hourly or shorter periods (radians) and t_1 is the length of calculation period.

The solar length time (ω) was determined using Equation 3.6 as:

$$\omega = \frac{\pi}{12}[(t + 0.06667(L_z - L_m) + S_c) - 12] \tag{3.6}$$

where t is the clock time at midpoint of period (hours), L_z is the longitude at the centre of the local time zone (radians), L_m is the longitude at measurement site (radians) and S_c is the seasonal correction for solar time (hour).

The seasonal correction for solar time (S_c) is defined by Equation 3.7.

$$S_c = 0.1645 \sin(2b) - 0.1255 \cos(b) - 0.025 \sin(b) \tag{3.7}$$

And b is determined using Equation 3.8

$$b = \frac{2\pi(J - 81)}{364} \tag{3.8}$$

where, J is the day of year.

To determine the daylight hours (N), Equation 3.9 was used.

$$N = \frac{24}{\pi}\omega_s \tag{3.9}$$

where, ω_s is determined using Equation 3.10.

$$\omega_s = \arccos[-\tan(j)\tan(d)] \tag{3.10}$$

where, j is the latitude (radians) and d is the solar decimation (radians)

Latitude (φ) was determined using Equation 3.11.

$$\varphi = \frac{\pi}{180} \times decimal\ degrees \tag{3.11}$$

The value for solar declination (δ) can be calculated from Equation 3.12.

$$\delta = 0.409\sin(\frac{2\pi}{365} \times J - 1.39) \tag{3.12}$$

where, J is the Julian day.

A number of weather stations were identified in and around the image to provide an accurate spatial representation of the meteorological data. This was done by projecting the location of the SAWS stations using Google Earth as depicted in Figure 3.5. The boundaries of the image scene was used as a guide to select the SAWS stations. Figure 3.6 provides a representation of the location of the SAWS stations in respect to the Landsat image scene for the Grasslands biome. Between four to six stations were identified for each biome.
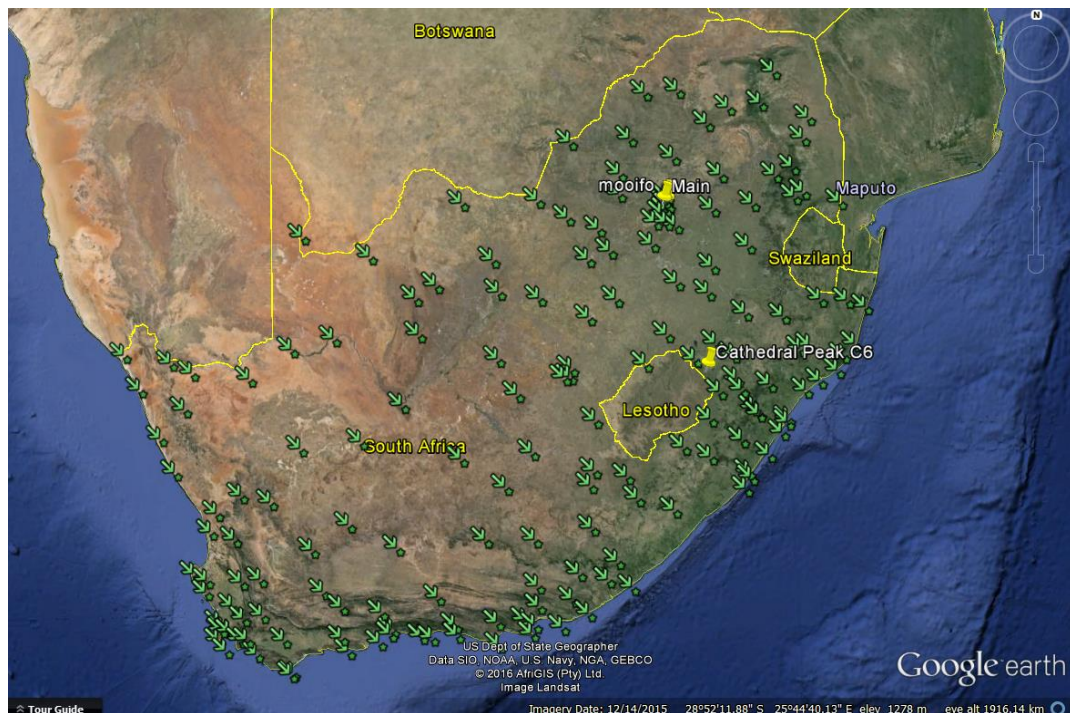

Figure 3.6   Location of SAWS stations around South Africa (Google Earth, 2016)
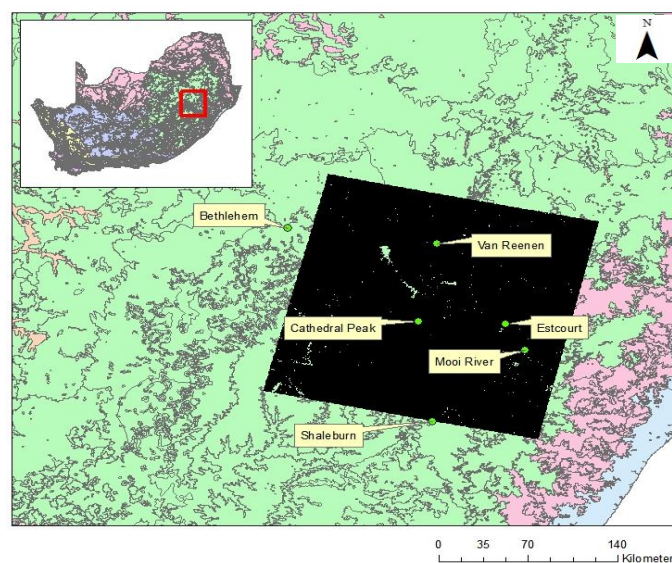

Figure 3.7   Location of SAWS in respect to Landsat image for grasslands biome

36

3.3.2   Determining large scale meteorological data maps

The meteorological data obtained from SAWS were point-based estimates. Since the entire Landsat scene was needed to provide a large scale estimate of ET, the meteorological data needed to be representative of the entire area.   Therefore, an interpolation method was applied to provide a spatial representation of the data to cover the entire image. The kriging technique available in ArcGIS was selected for this process. Figure 3.7 illustrates the result of the kriging technique applied over the Grassland biome. This technique was applied to all the meteorological data for all the biomes.
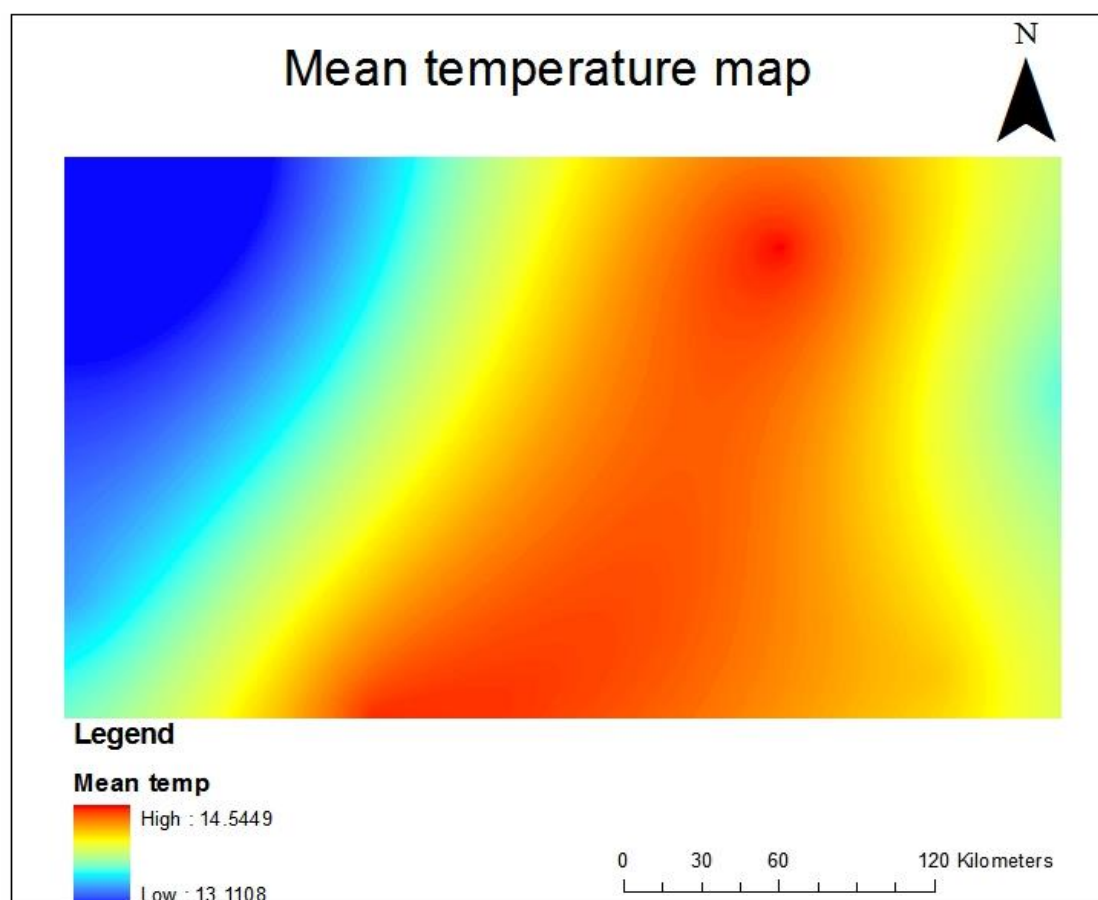

Figure 3.8   Result of kriging interpolation technique for mean temperature

The interpolated data was converted from ASCII to a raster format, using ArcGIS, which is compatible for processing in the SEBS model. The raster maps were imported into ILWIS and were ready to be used in the SEBS processing. The pre-processing of the data remained the same as explained in sub-section 3.2.2.

3.3.3 SEBS processing and ET extraction

The input data is the same as described in Figure 3.4. The only difference is the meteorological data maps are used instead of point-based estimates. The ET output maps produced were exported into ASCII format using the GDAL tool in ILWIS. A map depicting the land use of South Africa was obtained from the South African National Biodiversity Institute (SANBI). The map was projected in ArcGIS and areas which contained natural vegetation were extracted. This was done using the 'Clip' function in ArcGIS. The biome map by SANBI (2012) was projected and the biomes were clipped according to natural vegetation. The new map contained natural vegetation within a specific biome. The SEBS daily ET map was projected over the new map and the zonal statistic function in ArcGIS was used to obtain mean daily ET for each biome. This process was applied to all the images for all the biomes to extract mean daily ET.

Following the application of the model, statistical analysis was undertaken on the ET data obtained from SEBS to interpret the results obtained. This helped to draw conclusions on the accuracy of ET obtained from SEBS compared to the *in-situ* ET data as well as understand the seasonal variation of ET between the biomes. These results are presented in the next Chapter.

4. RESULTS

This section presents the results of two of the research questions outlined in Chapter one. The SEBS ET is first validated against *in-situ* data acquired from various sites across the country. Following this, the model was used to determine ET for a period from 1 July 2014 to 30 June 2015 to show the seasonal variation of ET. The results from this investigation are discussed in the latter part of this chapter.

4.1 Validation of the SEBS model across the South African Biomes

4.1.1 Grassland Biome

As stated in Chapter 3.2, ET estimates for Cathedral Peak were obtained using the eddy covariance technique and eight satellite images were processed in the SEBS model. The SEBS ET estimates fit the general trend of the eddy covariance ET measurements (Figure 4.1). The SEBS ET and the *in-situ* ET estimates were low during the winter month of July and gradually increased towards the summer months of November, December, January and February. The trend was similar between the SEBS ET and *in-situ* ET estimates during the cooler months of March and July. The SEBS ET estimates managed to capture the seasonal variation by producing low estimates in the cooler months and higher ET estimates in the warmer months. The SEBS model however, tends to over-estimate ET in comparison to the *in-situ* method throughout the study period except in the months of July and December where a close relation between the SEBS and *in-situ* measurements is observed.

The coefficient of determination (R^2) was determined. A R^2 value close to one represents a good correlation between the two data sets. In this instance an R^2 value of 0.81 was attained. Although this value is close to one, it needs to be considered in conjunction with the time series graph (Figure 4.1) which showed that the SEBS model over-estimates ET compared to the Eddy covariance system. The slope and intercept of the linear regression equation needs to be considered as well as the root-mean-square error (RMSE). A slope with a value close to one and an intercept with a value close to zero indicates a good correlation between the two data sets. In this case the slope and intercept values were 0.98 and 0.88, respectively. The RMSE is the measure of the difference between the sample (*in-situ* ET) and the modelled (SEBS ET) data. For this dataset a RMSE of ±1.1 mm.day^{-1} was attained.
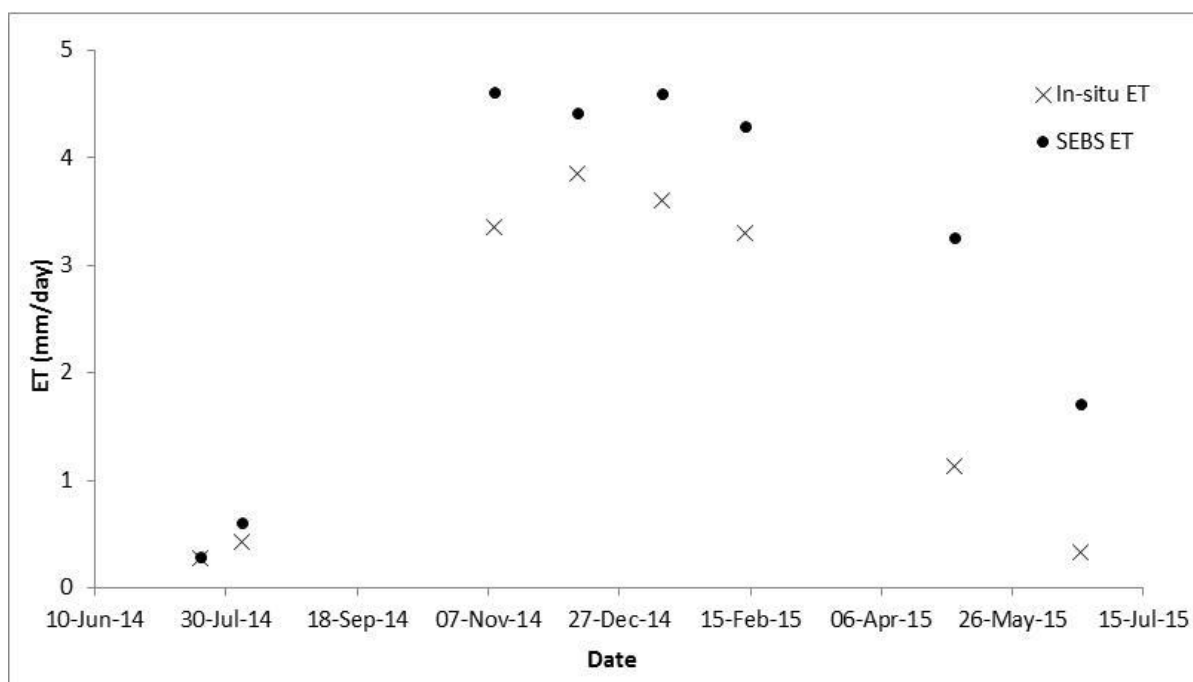
Figure 4.1   Time series graph between *in-situ* ET measurement and SEBS ET estimates of grassland vegetation from the Cathedral Peak research catchment

4.1.2   Fynbos Biome

A boundary layer scintillometer (BLS 900, Scintec, AG, German) (Dzikiti *et al.,* 2014) was used to obtain *in-situ* ET for fynbos vegetation in the Elandsberg Nature Reserve. A total of 11 satellite images were attained. A time series of the ET data obtained using the SEBS model and the *in-situ* ET using the boundary layer scintillometer is shown in Figure 4.2

In general, the SEBS model slightly over-estimates ET in most cases except on two occasions (23 December 2012 and 24 January 2013) where the SEBS ET is slightly less than the *in-situ* estimate of ET. The SEBS ET estimates follow the trend of the *in-situ* ET measurements closely for the months between November 2012 and April 2013. This coincides with the summer season. Between the months of July and August there is a noticeable difference between the ET estimates where the SEBS model over-estimated ET by close to 90% (1.1 mm/day). This could be a result of cloud cover as this is a winter rainfall area. During the month of October the correlation between the two methods of ET estimates are similar.
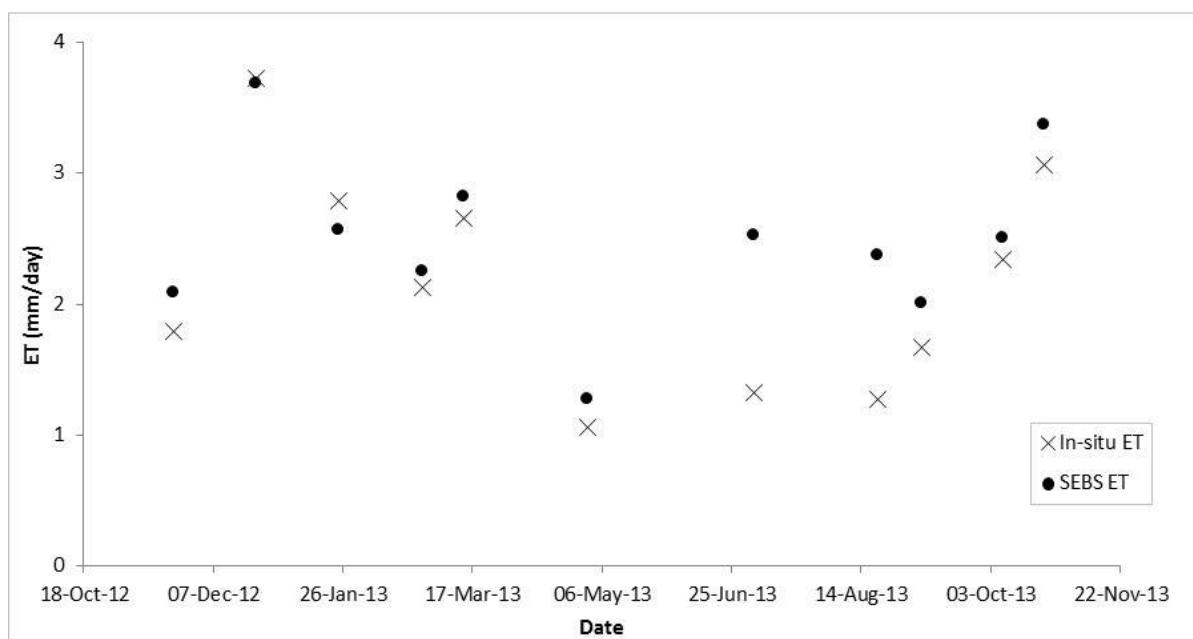
40

Figure 4.2   Time series graph between *in-situ* ET and SEBS ET for fynbos vegetation
from the Elandsberg Nature Reserve

The regression analysis produced a R^2 value of 0.73 . This indicates a good correlation between the two data sets. It is evident from Figure 4.2 that there is a poor correlation between the *in-situ* ET and SEBS for the winter season. This was confirmed by the R^2 that was calculated to be 0.56 for the winter period. For the summer season an R^2 of 0.87 was determined. The slope was 0.66 and the RMSE was calculated to be ±0.5 mm.day^{-1}. The poor correlation could be the result of cloud-cover as this is a winter rainfall area. This could have been the reason for the slope value of 0.66 and intercept of 1.06.

4.1.3   Savanna Biome

In-situ ET measurements using the eddy covariance system at the Skukuza were obtained for the period 26 July 2013 to 26 May 2014. The ET estimates from the SEBS model follows the same trend as the *in-situ* data (Figure 4.3). The SEBS and *in-situ* ET values are low in the winter months (July and August) and start to increase from October. The daily ET values peak in January with a maximum of 5.57 mm and 6.79 mm for the *in-situ* and SEBS estimates, respectively. The values start to decrease from mid-February till June. The lowest daily ET recorded by the eddy covariance system was 0.49 mm. The results from the SEBS model indicate a good correlation in capturing the seasonal variations. The SEBS model lowest estimate was for the same day, with an estimate of 0 mm. A regression analysis for the

41

in-situ and SEBS ET estimate produced a R^2 value of 0.7. The slope value was 1.34 with a RMSE of ±1.9 mm.day^{-1}.

Although the SEBS ET estimates follow the seasonal variations relatively well, the model tends to over-estimate ET. During the months of July, August and September the models ET estimates are similar to the *in-situ* data with the model underestimating on two occasions. For the rest of the data set the model over-estimates ET with larger differences between the two data sets.
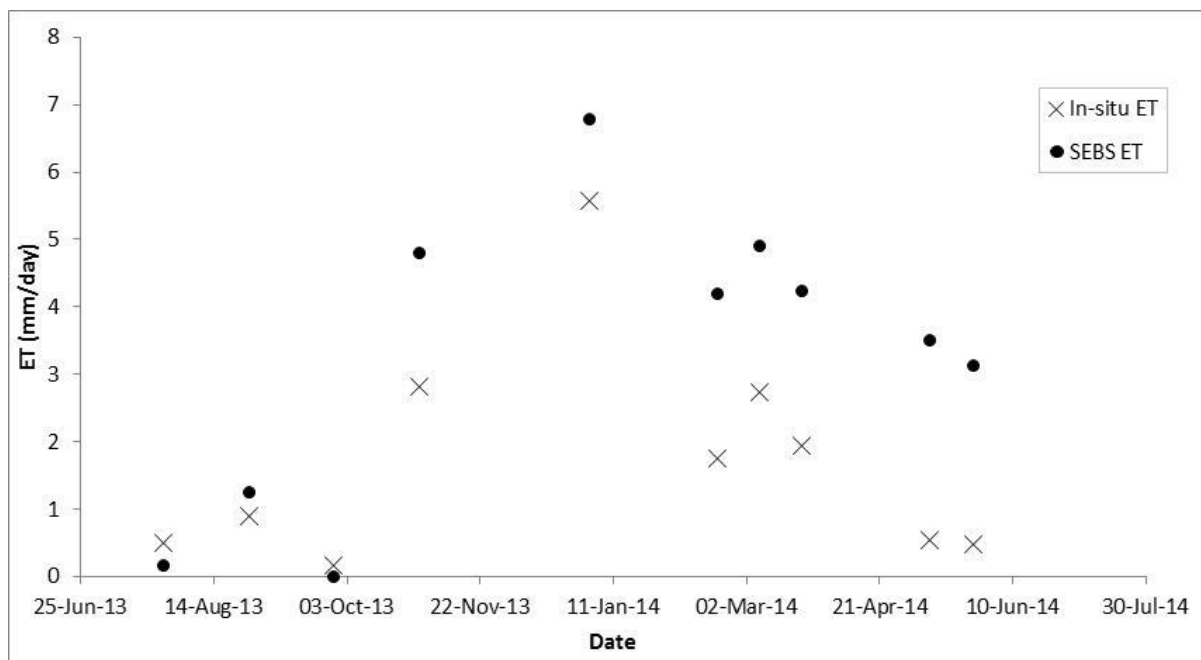
Figure 4.3   Time series graph between *in-situ* and SEBS ET estimates for Savanna
                vegetation at the Skukuza site

4.1.4   Forest Biome

The *in-situ* ET estimates for the vegetation representing the forest biome was attained using a CSAT3 Eddy covariance system (Gush and Dye, 2015). Due to the temporal resolution and cloud cover during the summer period the number of images for this site was limited to four images. The SEBS ET estimates mimicked the trend of the *in-situ* ET estimates. The ET from both sources increased from December and peaked in January 2013 before it decreased slightly at the end of the month. Although the trend was similar between the SEBS ET and *in-situ* ET estimates there is however, a consistent over-estimation of the SEBS ET (Figure 4.4).

A R^2 value of 0.78 was attained which indicates a good correlation between the observed and SEBS estimate of ET (Figure 4.4). However, a slope of 1.15 and intercept of 1.66 was attained. The intercept value does not correspond to a good correlation. An the RMSE was calculated to be ±2.24 mm.day^{-1} which is slightly high.
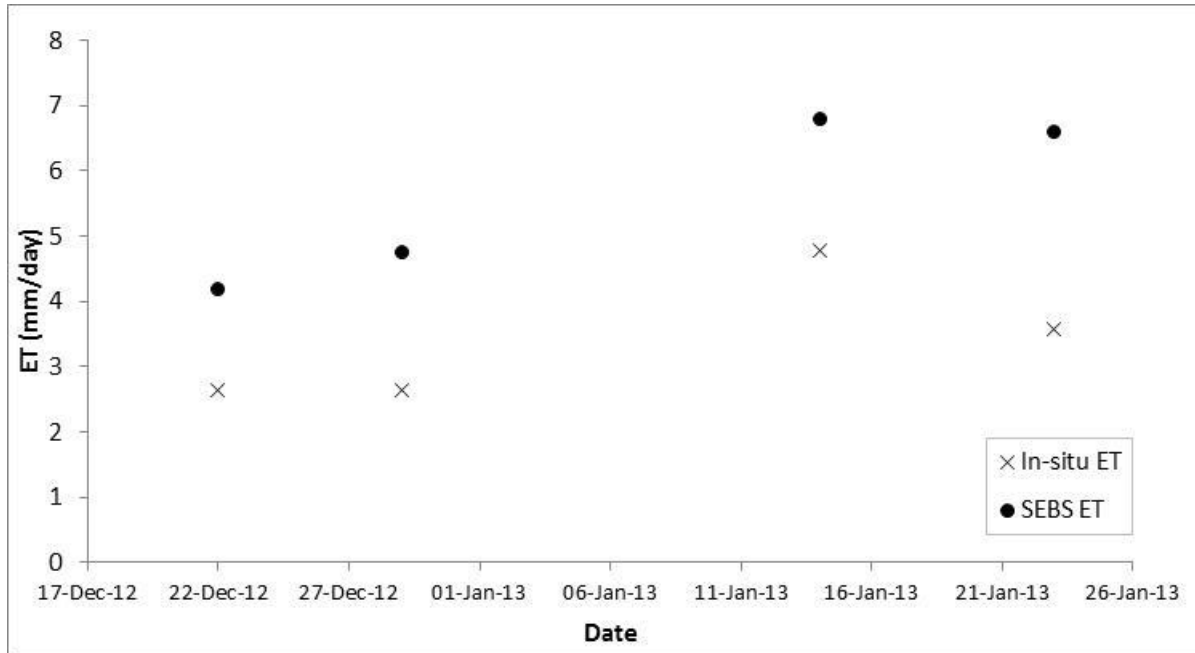
Figure 4.4   Time series graph between *in-situ* ET and SEBS ET for forest vegetation from the Ingeli State forest site

4.1.5   Indian Ocean Coastal Belt Biome

Measurements of ET were taken using CSAT3 Eddy covariance system. For this site three Landsat 7 ETM+ images were processed.

The results indicate a similar trend between the SEBS ET estimates and the *in-situ* ET measurement (Figure 4.5). The ET values were low in early September, following winter, and increased and peaked in February during the summer season. The ET estimates obtained using the SEBS model and the Eddy covariance system both decreased in May which is the winter season. SEBS marginally under-estimated ET in September and May, however, for February the model over-estimated ET with a larger difference between the values. An R^2 value of 0.99 was attained for this site (Figure 4.10). This indicates a good correlation between the *in-situ* and SEBS ET, however, it must be viewed in conjunction with the

regression statistics which produced a slope of 1.7 and an intercept of -1.5. These values are far from the recommend slope of 1 and intercept of 0.It is noted that the model tends to under-estimate ET in this case, however it must be remembered that this is based on three points.
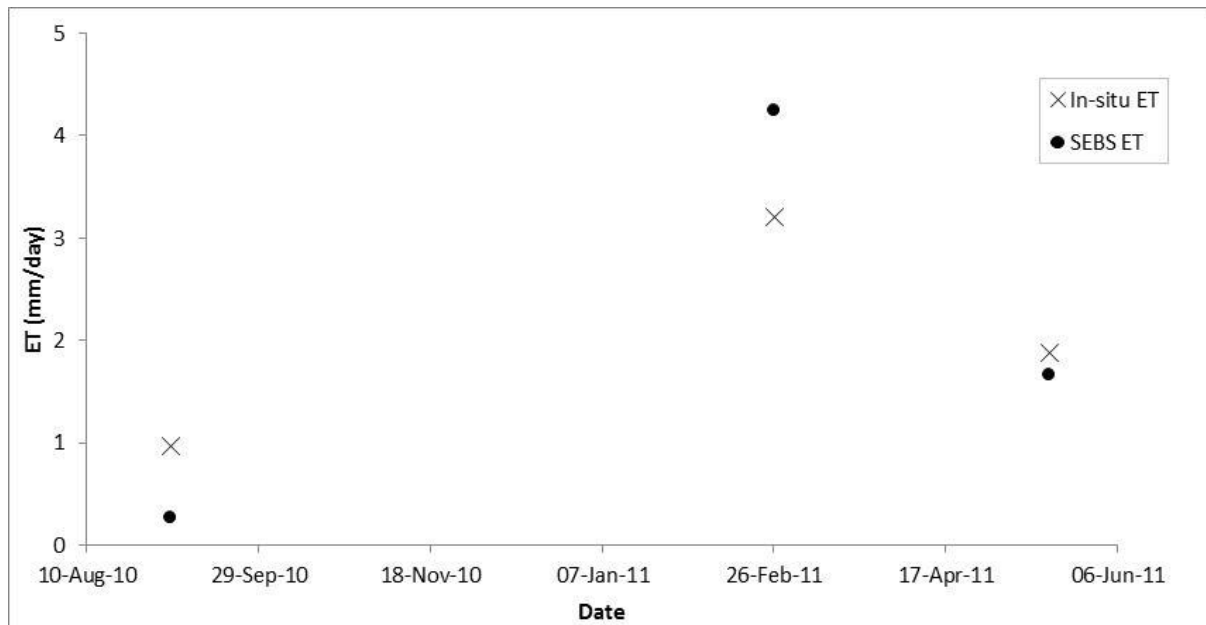
Figure 4.5   Time series graph between *in-situ* ET and SEBS ET for Indian Ocean Coastal Belt vegetation from the Manubi site

4.1.6   Nama Karoo Biome

In-situ ET data (obtained using a scintillometer) for the Nama Karoo biome was limited to a week. This resulted in only one satellite image being available on the 7 January 2008. There was a close comparison between the *in-situ* ET and the SEBS ET with the SEBS estimate being slightly lower. An *in-situ* ET value of 2.8 mm.day^{-1} was recorded and a SEBS estimate of 2.3 mm.day^{-1} was determined. This resulted in a 0.5 mm.day^{-1} difference between the two values which can be considered a good result however one image is not sufficient to confirm the accuracy of the two data sets.

4.1.7   Albany Thicket Biome

Only one image was available for the Albany Thicket biome, dated 27 September 2008. For this site the satellite based ET estimate was recorded to be higher than the *in-situ* ET

(obtained using an eddy covariance system). A value of 0.79 mm.day^{-1} was measured by the ground-based instrument whereas the SEBS model estimated a daily ET value of 1.5 mm.day^{-1}. This indicates an over-estimation by the SEBS model with the ET value being twice as high as the *in-situ* measurement. Due to the lack of sufficient satellite images it is difficult to draw a sound conclusion on the accuracy of the SEBS ET estimates.

4.1.8 Comparison of validation results across all sites

Given the limited number of points (images available corresponding to available observed ET data) available for validation, a comparison of the *in-situ* ET measurements to the satellite-based ET estimates across the sites was made. A regression graph was plotted and a R^2 value of 0.66 was obtained (Figure 4.6).
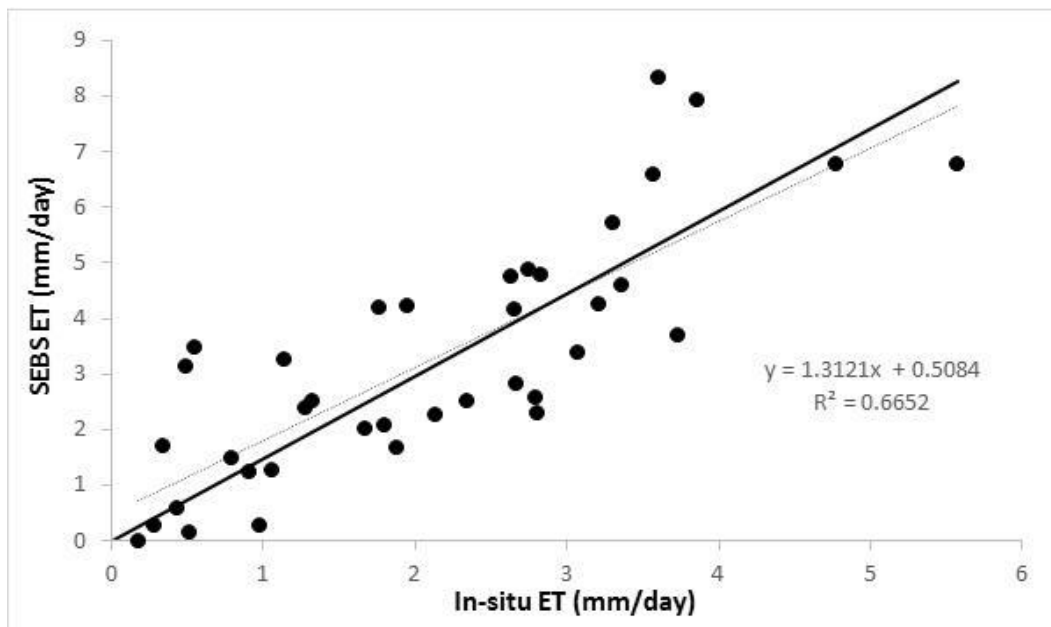
Figure 4.6   A regression graph including all *in-situ* data from the various sites vs. SEBS modelled ET

The RMSE was determined to be ±1.7 mm.day^{-1}. The R^2 and RMSE value was significant enough to conclude that an adequate comparison is present between the *in-situ* ET and SEBS ET estimates given the insufficient images in general across the sites, and in particular for the Nama Karoo and Albany Thicket biome. The specific problems identified at the various sites must be noted, for example, the summer period in the Grasslands biome and Indian Ocean

Coastal Belt, the winter period in the Fynbos biome and throughout the Forest biome the SEBS ET estimates were higher than the *in-situ* measurements. During the winter months, specifically the Grassland and Indian Ocean Coastal Belt biome the difference between the SEBS ET and *in-situ* ET was minimal. This is the opposite case regarding the Fynbos biome as the dry season estimates showed minimal difference compared to the wet months which showed a larger difference.

4.2   Estimating ET using the SEBS model

The first stage in modelling the ET was to compute hourly solar radiation using the equation by Allen *et al*. (1998) as described in Chapter 3. The modelled solar radiation was compared to *in-situ* measured solar radiation obtained from the Elandsberg Nature Reserve by Dzikiti *et al.* (2014). The *in-situ* solar radiation was measured using a pyranometer (Dzikiti *et al.*, 2014).

The time series graph (Figure 4.7) of *in-situ* and modelled solar radiation data shows that the modelled and observed data follow the same trend. The solar radiation is high at the beginning of the year during the summer months as expected and gradually decreases towards the winter season before increasing again during spring and into the summer season. However, the modelled solar radiation data is consistently higher and less variable than the *in-situ* data (Figure 4.12). The regression analysis produced a R^2 of 0.82. However, it is evident from the intercept (426.07)and slope (0.62) that is not a good simulation.
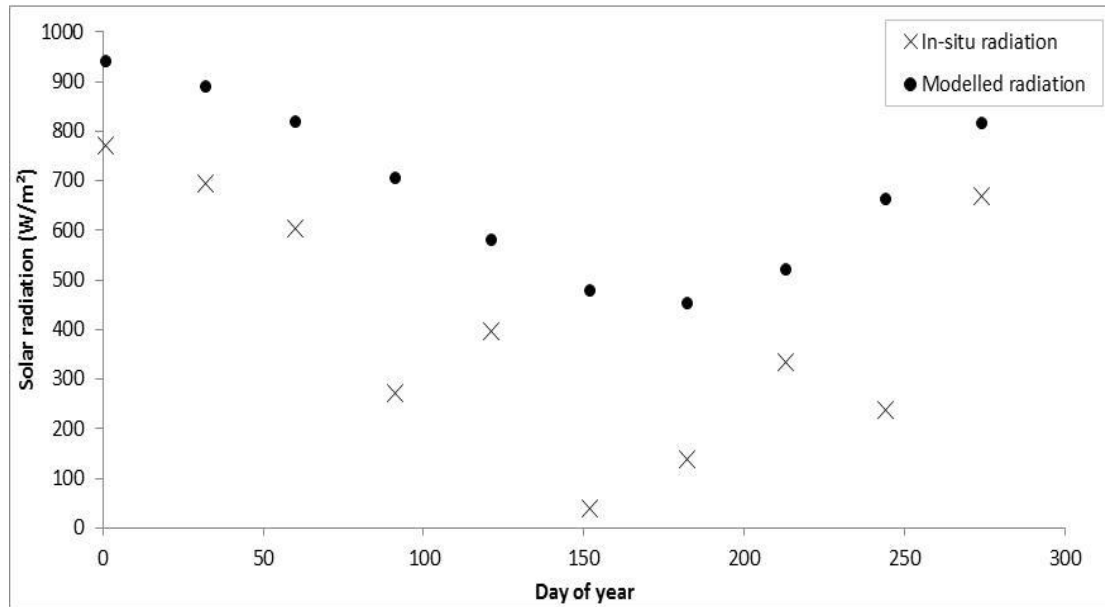
Figure 4.7 Time series graph of hourly *in-situ* solar radiation versus hourly modelled solar radiation using the equation the equation by Allen *et al.* (1998)

Images were downloaded for the year long period 1 July 2014 to 31 June 2015 for the seven biomes. The number of images obtained (Table 4.1) were limited by cloud cover and the availability of meteorological data. Measured meteorological (air temperature, pressure and wind speed) data was obtained from SAWS and solar radiation was computed, using the hourly solar radiation model by Allen *et al*. (1998).

The solar radiation and air temperature for the various biomes is shown in Figure 4.8 as they have a significant influence on the SEBS model in estimating ET. For each biome a number of sites were identified to provide an accurate spatial coverage. The average value from the various sites was used in Figure 4.15. The Nama Karoo biome experiences the lowest solar radiation with all values below 400 $W.m^{-2}$. The rest of the biomes experience a minimum solar radiation between 500 $W.m^{-2}$ to 600 $W.m^{-2}$ and a maximum between 900 $W.m^{-2}$ to 1000 $W.m^{-2}$. The minimum solar radiation is experienced in the winter months and peaks in the summer season.

Figure 4.8   Solar radiation, air temperature and ET data for the various biomes

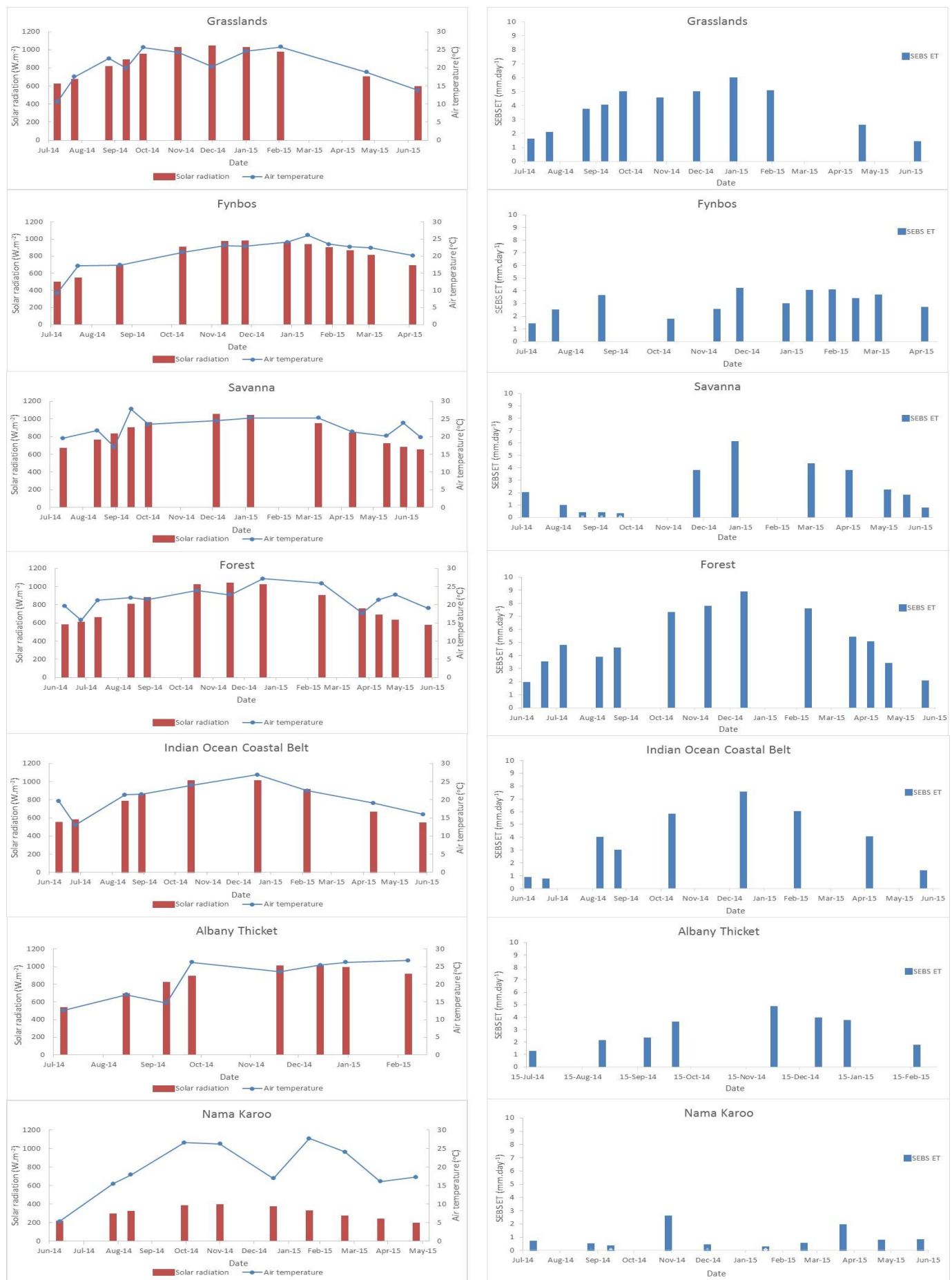The air temperature at satellite overpass time is shown in Figure 4.8. The average from the various sites within the biome was used in the above graphs. The maximum values were between 25°C and 28°C whereas the minimum values are between 5°C and 18°C. The highest temperature was experienced by the Savanna biome followed by the Nama Karoo and Forest biome. The lowest air temperature values were experienced in the Nama Karoo biome followed by the Fynbos and Grasslands biome.

The highest daily ET value of 8.7 mm was obtained for the Forest biome on the 12 January 2015 and the lowest daily ET estimate of 0.09 mm on the 17 January 2015 for the Nama Karoo biome (Table 4.1). The model produced the highest mean ET value of 4.9 mm.day^{-1} for the Forest biome and the lowest mean ET value of 0.71 mm.day^{-1} for the Nama Karoo biome. For the Fynbos and Albany Thicket biomes, similar mean ET values of 2.88 mm.day^{-1} and 2.75 mm.day^{-1}, respectively were estimated. The minimum modelled ET values for all the biomes are below 2 mm.day^{-1} whereas the maximum values vary from 2.40 mm.day^{-1} to 8.70 mm.day^{-1}. The Grassland, Fynbos, Albany Thicket, Savanna and Indian Ocean Coastal Belt modelled mean ET values fall within the 2-4 mm.day^{-1} range. The largest range in modelled ET values was obtained for the Forest biome with a difference of 6.94 mm.day^{-1} between the maximum and minimum daily ET values. The Indian Ocean Coastal Belt biome has the second largest difference of 6.79 mm.day^{-1} followed by the Savanna biome with a range of 5.83 mm.day^{-1}. The lowest range was for the Nama Karoo biome with a range of 2.32 mm.day^{-1} closely followed by the Fynbos biome with a range of 2.79 mm.day^{-1}.

Table 4.1   Maximum, minimum, mean daily ET values and range for each of the seven biomes

Biomes	Number of images	Maximum ET (mm.day^{-1})	Minimum ET (mm.day^{-1})	Mean ET (mm.day^{-1})	Range (mm.day^{-1})
Grasslands	11	5.80	1.26	3.55	4.55
Fynbos	12	4.01	1.22	2.88	2.79
Forest	13	8.70	1.76	4.90	6.94
Nama Karoo	10	2.40	0.09	0.71	2.32
Albany Thicket	8	4.65	1.07	2.75	3.57
Savanna	12	5.93	0.10	2.09	5.83
Indian Ocean Coastal Belt	8	7.34	0.55	3.81	6.79

A time series graph representing the SEBS ET estimates for the biomes is shown in Figure 4.9. The Forest biome has the highest modelled ET throughout the year, with the highest summer and winter ET estimates of 8.7 mm.day^{-1} and 1.76 mm.day^{-1}, respectively. The Nama Karoo biome has the lowest modelled ET values throughout the year with values below 0.6 mm.day^{-1} in most instances except for 29 October 2014 and 22 March 2015 where the modelled ET estimates are 2.4 mm.day^{-1} mm/day and 1.7 mm.day^{-1}, respectively. The Forest, Grassland, Fynbos, Albany Thicket, Savanna and Indian Ocean Coastal Belt biomes follow the same seasonal trend with lower ET values in the winter months and gradually increasing towards the summer season and then decreasing again in the winter months. For the month of September a number of biomes experienced low ET rates.
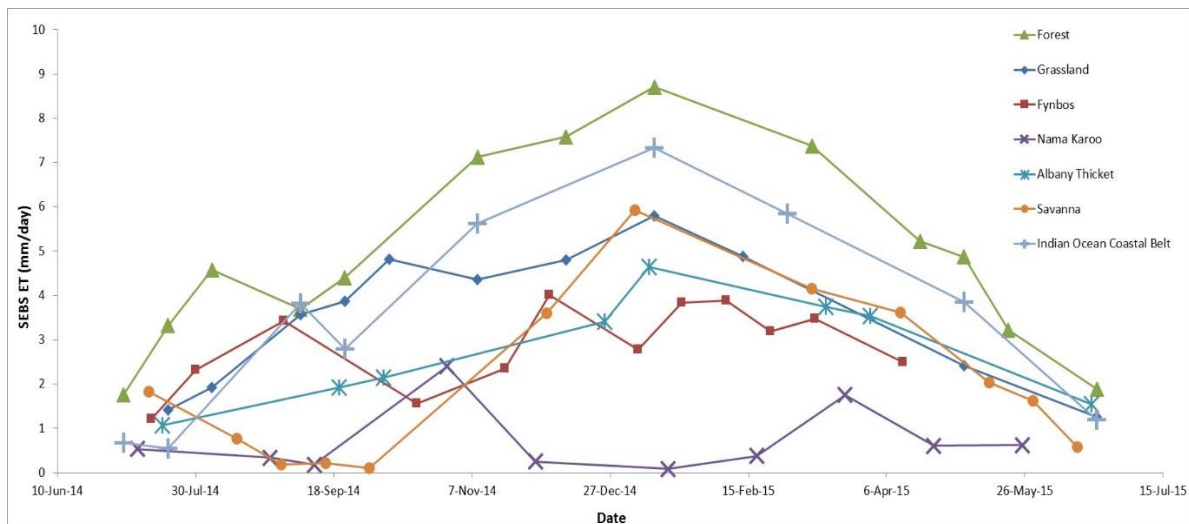
Figure 4.9 Time series graph of modelled SEBS ET estimates for the seven biomes for July 2014 to June 2015

An example of ET maps for each biome is shown in Figure 4.10. It is evident that there is a high degree of variation within each biome except for the Savanna biome. For the Savanna biome the ET is fairly constant except for a few dark patches, which indicate lower ET values. Higher ET values are estimated along the eastern shoreline as depicted in the images covering the Indian Ocean Coastal Belt and Albany Thicket biomes. The image covering a portion of the Grasslands biome indicates higher ET estimates at the higher altitudes.
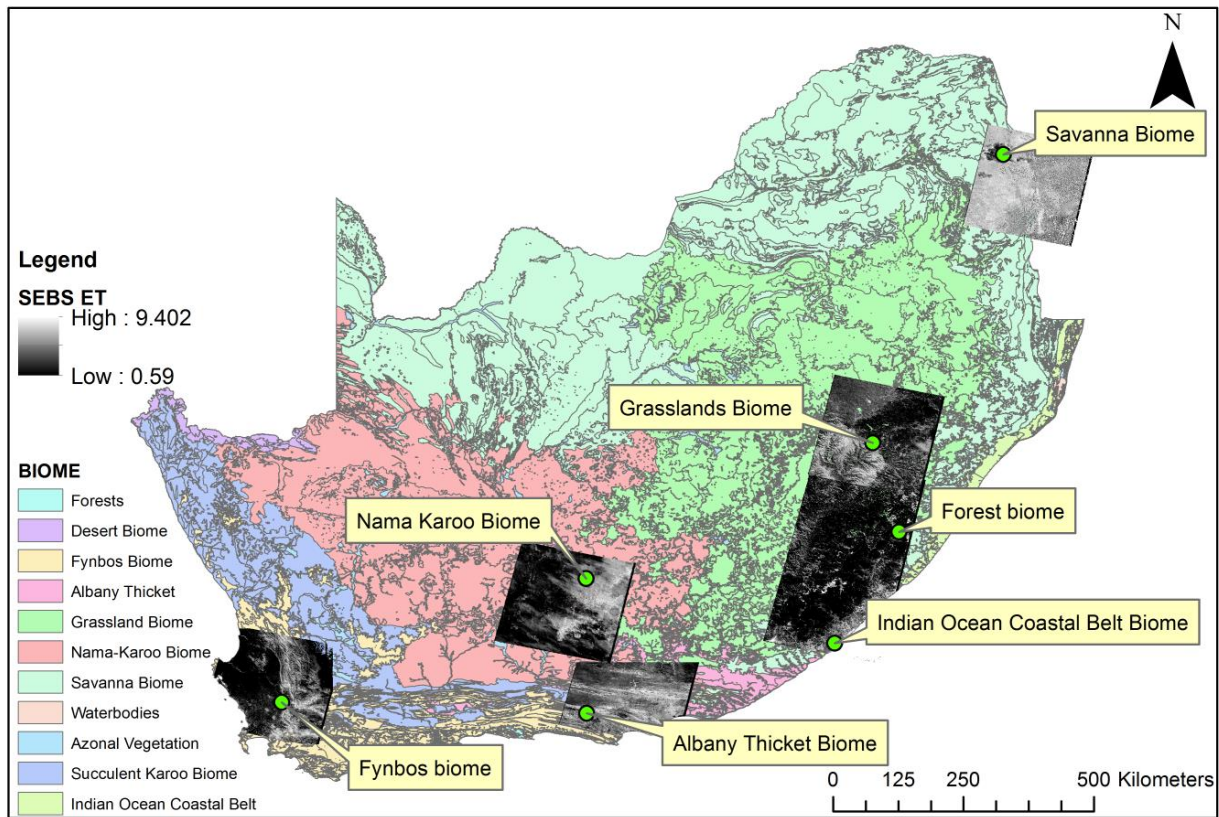
Figure 4.10   Example of SEBS ET map for the seven biomes

The SEBS ET estimates followed the trend of the *in-situ* ET data fairly well for the validation study. The comparison between all the *in-situ* ET and SEBS ET yielded a R^2 value of 0.66 and a RMSE of ±1.7 mm.day^{-1}. However, there seems to be an over-estimation of SEBS ET compared to the *in-situ* ET data. The modelling of ET for a year-long period showed the seasonal variation through the months as well as the variation of ET between the biomes. The next chapter focuses on the discussion of the results.

5. DISCUSSION

The advent of remote sensing has made it possible to estimate ET at a larger spatial scale than *in-situ* methods. The SEBS model made it possible to estimate ET for the different biomes. This study, first investigated the accuracy of the SEBS model when compared to *in-situ* ET estimates and then used SEBS to model ET for a year over the seven biomes to understand the seasonal and spatial variation of ET across the biomes.

5.1 Comparison of SEBS ET to *in-situ* ET

The ET estimates obtained from SEBS followed the seasonal trend well for the five biomes where several images could be processed and validated. Majority of the sites were located in a summer rainfall region. The ET produced from SEBS was lower in the winter months and increased in the summer season, which was consistent with the *in-situ* data. This could be a result of higher the atmospheric evaporative demand in the summer season compared to the winter season. Another reason could be the higher rainfall present in the summer season compared to lower rainfall experienced in the winter season. However, the Fynbos site experiences winter rainfall. The model over-estimated ET during this period which could be a result of enhanced biophysical characteristics (NDVI, LAI LST, FVC) present in the vegetation due to water availability or the impact of cloud cover.

A R^2 value of 0.66 was attained for the data across all sites. This value is low compared to an R^2 of 0.84 and 0.81 attained by Elhag *et al.* (2011) and Singh and Senay (2016), respectively, for estimates of ET over agricultural fields. It needs to be noted, however, that the SEBS model was initially developed for agricultural landscape (Gibson *et al*. 2013). Thus, due to the models parameterization of roughness length, a better correlation between *in-situ* and SEBS ET is typically achieved over agricultural areas (Elhag *et al.,*2011; Gibson *et al*., 2013) and a poorer correlation attained over varying land cover (van der Kwast *et al*., 2009). However, several studies over natural vegetation have shown that SEBS is able to produce reliable estimates of ET (Rwasoka *et al.*, 2011; Ma *et al*., 2014; Shoko *et al*, 2015a and Shoko *et al.*, 2015b). This study further added to the evidence that SEBS is able to estimate the ET of natural vegetation, with a R^2 of 0.81 for grasslands, a R^2 of 0.73 for fynbos, a R^2 of

0.78 for forest. The Nama Karoo and Albany Thicket biome was limited by satellite images, hence the R^2 could not be determined.

Overall, the SEBS model over-estimated ET in comparison to the *in-situ* data. This finding was similar to the findings of Rwasoka *et al.* (2011) and Singh and Senay (2016) for work done over grasslands and to Shoko *et al.* (2015) and Zhuo *et al.* (2014) over forests. Rwasoka *et al.* (2011) explained that the reasons for the over-estimation could be a result of land surface heterogeneity, the variability of air temperature data and roughness parameterization. Mamo (2010) agreed that the influence of land surface heterogeneity has an effect on ET, especially in arid and semi-arid regions. This finding is further supported by Gibson *et al.* (2011, 2013) and Shoko *et al.* (2015). Thus, the influence of spatial heterogeneity should be considered when using the SEBS model to estimate ET. In this study, the Landsat image covered a large area of each biome. The size of the image scene is approximately 170 km by 185 km (USGS, 2015). This means that a number of vegetation units (defined by SANBI, 2012) were present in the image scene. The Landsat image that covered the Fynbos biome consisted of approximately 59 different vegetation types. A total of 25 and 23 vegetation types were found within the Grasslands and Albany Thicket biome, respectively. This gives an indication of the variation in land cover in each biome. The number of vegetation types, equating to land heterogeneity, present in the biomes could explain the over-estimation. Other reason for the over-estimation of ET could be related to the fact that the model assumes the conditions experienced when the image is captured are experienced throughout the day. The Landsat satellite passes South Africa around midday when air temperature and solar radiation is at the peak for the day. The high temperature and solar radiation is assumed for the whole day hence producing high daily ET resulting in an over-estimation.

The *in-situ* ET data was obtained using an eddy covariance system and scintillometer. The SEBS model produced better estimates of ET when compared against the *in-situ* ET attained using the scintillometer for the Fynbos validation site. A RMSE of 0.5 mm.day^{-1} was attained for this investigation. The reason could be attributed to the larger spatial coverage by the scintillometer. The largest difference was attained using an eddy covariance system, for the Forest biome with a RMSE of 2.24 mm.day^{-1} however, there were only four images available for this site. The eddy covariance system covers a much small spatial area which may explain this difference in ET. SEBS did provide some degree of confidence to model ET for a year

especially for the Grasslands and Fynbos biome as there was sufficient images to validate the model and the RMSE was determined to be 1.1 mm.day^{-1} and 0.05 mm.day^{-1}, respectively.

5.2   Spatial and Seasonal Variation in ET

Seasonal changes in ET are attributed to the vegetation and climatic characteristics. The highest ET estimate was produced in the summer season whereas lower estimates are experienced in the winter period. This could be related to the different rainfalls experienced. The maximum ET for the wet and dry season was produced for the Forest biome. This is likely as forests have deep root systems which are able to extract groundwater in the dry season (Zhang *et al*., 2001). Forests also have a larger canopy cover than the other vegetation allowing it to intercept more water and hence evaporate more. The Nama Karoo biome had the lowest ET estimates for the wet and dry periods. This could be attributed to the fact that the interior of South Africa receives the least amount of rainfall. According to van der Kwast *et al.* (2009) the SEBS model tends to under-estimate H in dry areas and where vegetation is sparely disturbed, whereas Workineh *et al*. (2016) found that the SEBS model produces higher estimates of ET in areas with high vegetation cover. This was evident in this study, with the Forest, Fynbos, Grasslands, Indian Ocean Coastal Belt and Savanna biomes which have good vegetation cover recording high mean ET. On the other hand, the lowest mean ET was modelled for Nama Karoo biome where the dominant vegetation is dwarf shrubland which is generally sparsely distributed (SANBI, 2016). Similarly, Rwasoka *et al.* (2011), Zhuo *et al.* (2014) and Shoko *et al.* (2015) reported that forest plantations recorded the highest ET followed by grasslands and the lowest ET rates were obtained from bare soils and areas with little vegetation cover. Furthermore, the SEBS ET estimates for the Forest biome had the highest minimum ET during the winter season.

As mentioned above, the SEBS model is highly sensitive to air temperature (Su, 2002, Badola, 2009; van der Kwast *et al*., 2009). The temperature gradient has a direct impact on the calculation of sensible heat flux, which is used in SEBS to ultimately determine ET, therefore the changes in temperature have an influence on ET. This is evident in the validation and modelled ET results. During the summer season when air temperature is high there is an increase in SEBS ET whereas during the winter season the SEBS ET is lower. The sensitivity of SEBS to air temperature is further evident in the month of September where the

54

modelled ET value is low for the Forest, Indian Ocean Coastal Belt and Savanna Biomes (Figure 4.15). During the same period it is evident that the air temperature at these sites is low (Figure 4.14). The influence of air temperature is seen again for the Nama Karoo biome for the month of January. Although the solar radiation values were reasonable, the temperature for that month is low which produces a lower ET (Figure 4.14). For the Grasslands biome the lower air temperature for December coincides with a lower ET (Figure 4.14). For the modelling component of this study the solar radiation is produced using a model, therefore, the fluctuations in radiation and its impact on ET is negligible as a gradual increase from the winter to summer months is experienced. This therefore highlights the influence of temperature on the ET estimation using SEBS.

Overall, the model was able to capture the seasonal variation of the biomes as well as the variation of ET between the different biomes. The general trend of higher ET was evident in the wet season and lower ET in the dry season. The Forest biome was expected to produce the highest ET due to its biophysical characteristics (deep roots, large canopy). The Grasslands biome had the second highest ET. This could be as the Grasslands biome is situated on the eastern side of South Africa. This area receives the highest MAP for the wet season. The limitation of rainfall in the Nama Karoo biome was evident with the model ET results produced.

5.3   Remote sensing of ET as an approach to determine water use for vegetation clusters

The focus of the research project was to develop a methodology that could be used to determine the water use input parameters from the natural vegetation clusters. In order to do this the ET_c, ET_o and K_c values are required. The ET_o can be determined using the method developed by the Food and Agricultural Organisation (FAO) which is commonly referred to as the FAO Penman-Monteith (Allen *et al.,* 1998). This study focused on a methodology to determine the ET_c which can be used, along with ET_o, to determine K_c, using Equation 2.7. K_c values are used as inputs in hydrological models. ET_c will be referred to as ET in this discussion.

Accurate estimates of ET are required to produce reliable K_c values. *In-situ* methods are regarded as highly reliable techniques to determine ET. However, the limitations relating to

the spatial coverage and mobility of these instruments make it difficult to estimate ET over various vegetation covers. The application of satellite remote sensing has the ability to overcome these challenges. However, the confidence to use remote sensing to estimate ET needs to be justified. This can be achieved by comparing the *in-situ* ET measurements using conventional techniques to the satellite derived ET estimates as investigated in this study. However, the use of different *in-situ* methods may compare differently to the satellite ET estimates. The scintillometer covers a larger transect compared to the eddy covariance which measure point-based ET. The remote sensing ET estimates over certain vegetation seems more reliable than others as discussed in Chapter 5.1. These include the grasslands, fynbos and savanna vegetation especially since a number of satellite images were available to validate ET. Therefore the water use of the vegetation clusters which fall within these biome regions can be estimated with a fair degree of accuracy. The SEBS ET estimates were in good correlation with *in-situ* ET measurements for the forest site however, only four images were available. The rest of the sites (Indian Ocean Coastal Belt, Nama Karoo and Albany Thicket) require a greater length of data to determine its accuracy.

The methodology adopted in this study to estimate ET does provide an opportunity to determine the water use of natural vegetation clusters using the SEBS model. The remote sensing of ET is able to produce large scale estimates of various vegetation types in much less time compared to *in-situ* techniques and over a number of vegetation types. The results from the study indicated that vegetation within the Grasslands, Fynbos, Forest and Savanna biomes produce fairly reliable estimates of ET. However, there was a general over-estimation of ET from SEBS. This would influence the calculation of K_c. In this instance an over-estimation of ET will result in an over-estimation of K_c. A method to overcome this would be to use a scaling factor to lower the estimate of SEBS ET and hence produce a more reliable estimate of K_c. Due to the lack of images available for the Indian Ocean Coastal Belt, Nama Karoo and Albany Thicket biome the accuracy of SEBS ET and hence the influence it has on K_c cannot be determined. Further investigation will be needed to assess the accuracy of SEBS ET in these regions.

6. CONCLUSION AND RECOMMENDATIONS

6.1 Conclusion

The advancement in technology has allowed scientists to acquire, analyse and provide sound conclusions to aid in decision and policy making. This study doesn't fall far from this premise. Given the scarcity of water, the planning and management of water resources require information with the highest of accuracy.

The portioning of water across various land covers has to be well understood in order to properly gauge its distribution and use. The response of water over various land cover is different, therefore a baseline land cover is required to assess and compare the use and response of water. Currently the Acocks' (1988) Veld Types is used as the baseline in South Africa. However, there has been an improvement in the acquisition and collaboration of land cover information across the country. The SANBI (2012) vegetation map provides a detailed description of the natural vegetation cover of South Africa. However, the water use parameters for this have not been determined. This study investigated a methodology that can be used to determine the ET which is required to determine water use parameters such as crop coefficients.

A review of the various methods to estimate ET (water use) was discussed. There were a number of limitations identified with regard to the *in-situ* methods to estimate ET. The advent of remote sensing overcomes many of these limitations. Remote sensing models are able to produce large scale estimates of ET at the fraction of the cost compared to *in-situ* methods. The ability to acquire ET estimates of the landscape without being in contact with is a value asset especially in large scale studies as such. In South Africa, the SEBAL and SEBS models have been widely applied. For the purpose of this study SEBS was the most suitable model to use. The methodology was separated into two steps to address the first two research questions.

Firstly, *in-situ* ET data was used to validate satellite derived ET using the SEBS model for several sites across the country to determine its accuracy. The sites were selected based on the availability of ET and meteorological data within each biome. The SEBS ET estimates follow the trend of the *in-situ* ET data well. The lower ET estimates were produced for the

dry season and higher ET estimates for the wet season. This was the case for the *in-situ* ET as well. The sites within the Grasslands, Fynbos and Savanna biomes had a number of satellite images available to validate the model with a degree of confidence. R^2 values of 0.81, 0.73 and 0.70 were attained for the sites within the Grasslands, Fynbos and Savanna biome, respectively. A regression graph was plotted and the number of data points above the 1:1 line indicate the over-estimation of the model for these sites. The reasons for the over-estimation could be a result of land surface heterogeneity, the variability of air temperature and roughness parameterization as SEBS was initially developed for agricultural landscape. Although, a number of studies applied SEBS over natural vegetation with a fair degree of accuracy indicating the models ability to estimate ET over natural vegetation. The rest of the *in-situ* sites did not have sufficient images and this affected the accuracy of the model.

Following the validation of SEBS the model was applied to estimate ET for between 1 July 2014 to 31 June 2015 for the seven biomes. This was done in an attempt to understand the spatial and seasonal variation of ET between the biomes. The modelling results indicated that the Forest biome produced the highest ET in the summer with a mean ET of 4.9 mm.day^{-1}.This could be the result of the biophysical characteristics (large leaf area index and deep root systems) of the forest vegetation. The lowest ET was produced for the Nama Karoo biome with a mean ET of 0.71 mm.day^{-1}. The scarcity of rain and presence of shrubland vegetation in this area could be the result of this finding. The largest biome in South Africa (Savanna biome) had a mean ET of 2.09 mm.day^{-1} followed by the Grasslands biome with 3.55 mm.day^{-1}. These biomes have a fair coverage of vegetation and are situated in the wetter region of the country which could attribute to the ET results obtained.

The modelling results highlighted SEBS sensitivity to air temperature. The temperature gradient has a direct impact on the calculation of sensible heat flux, which is used in SEBS to ultimately determine ET. Therefore, the changes in temperature have an influence on ET. High air temperature results in higher estimates of ET. The winter season experiences low air temperatures compared to the summer season. This trend was present for the ET estimates obtained from SEBS for the month of September, an isolated case, where low air temperature was experienced for a few biomes. This resulted in lower estimates of ET. The models sensitivity to solar radiation could not be expressed as a model was used to determine solar radiation since measured solar radiation was not available from the SAWS. The modelled

solar radiation gradually increased from the winter to the summer season with no significant fluctuations which would have an impact on the estimation of ET.

This dissertation was aimed at developing a methodology to estimate water use. Given that there are a number of vegetation clusters, this methodology can be applied to derive the water use which will be used to determine the water use parameters as highlighted as the third aim of the WRC project. However, the lack of meteorological data at certain sites will restrict the application of this method. The SEBS model provides a degree of confidence in estimating water use in the Grasslands, Fynbos and Savanna biomes. The model performed well in the Forest biome however, only four images were available. It is recommended that further investigation in the Indian Ocean Coastal Belt, Nama Karoo and Albany Thicket, biome, should be taken to assess the models accuracy to estimate ET.

Satellite derived ET using the SEBS model compared fairly well to *in- situ* ET in a few biomes. The spatial and temporal resolution of ET can be achieved using remote sensing. Overall, remote sensing proves a viable option to estimate ET over large areas. The SEBS model is cost-free and Landsat images are freely available. The estimates of ET for this study was produced from across the country without setting up instruments or taking physical measurements. Given that meteorological data is available for the prescribed sites, the estimation of ET is achievable. The use of remote sensing can be used to acquire precipitation, soil moisture and ET data with a degree of accuracy. This is valuable to authorities who require data over larger areas in a short space of time to provide insight in water related issues.

6.2   Limitations and Recommendations

The study can be improved by taking a few factors into consideration. A longer record of *in-situ* ET data is required to validate against satellite derived ET, especially over the Forest, Indian Ocean Coastal Belt, Nama Karoo and Albany Thicket biomes. Landsat has a temporal resolution of 16 days therefore approximately two images are available per month. For a validation study this is not enough. Cloud cover, especially during the rainy season further reduces the number of satellite images available. For sites with an ET record of two to three weeks, the influence of cloud cover in conjunction with the temporal resolution makes it

difficult to validate. An alternate satellite, for example MODIS, could be used since it has a daily temporal resolution however, the spatial resolution is compromised.

Landsat 7 ETM+ images have scan line which run across the entire image. If this satellite images are used for a validation study it is possible that the location of the *in-situ* instrument could fall within the scan line which contains no data. This will result in no ET estimation for the site. However, the scan lines are not more than three pixels so the pixel closet to the study site can be used as an alternative.

In-situ ET data for natural vegetation could not be attained for the Azonal and Succulent Karoo biomes. The measurement of ET using *in-situ* techniques can be conducted which would then provide an opportunity to investigate the accuracy of satellite derived ET from these biomes. The SEBS ET estimates compared better against the ET measurement obtained using a scintillometer than the eddy covariance. This could primarily be related to the larger spatial coverage by the scintillometer. Therefore future studies should consider using the scintillometer to estimate *in-situ* ET.

The SEBS model requires meteorological data such as wind speed, solar radiation, air temperature and pressure. This data can be obtained using an AWS. For the modelling investigation this data was required from a number of sites therefore the SAWS was selected to provide this data. However, measured solar radiation data was not available and a model by Allen *et al*. (1998) was used to estimate solar radiation which could have had an influence on the ET estimations. Instruments such as the pyranometer need to be installed at sites to provide actual measurements of solar radiation.

The SEBS model requires a number of inputs which is time consuming to attain especially when dealing with a number of study sites. In some sites not all of the data that is required is available therefore it has to be acquired from other sources. The *in-situ* data measured at sites are useful for various studies and application however, this data is difficult to access. A database should be developed where measured meteorological, ET or any other important data can be uploaded. This will reduce the amount of time spent searching for data.

7. REFERENCES

Acocks, JPH. 1953. *Veld Types of South Africa: With 5 small vegetation maps and accompanying Veld Type Map*. Botanical Survey Memoir No. 28. The Government Printer, Pretoria, South Africa.

Acocks, JPH. 1988. Veld Types of southern Africa. Botanical Research Institute, RSA. Botanical Survey of South Africa Memoirs, 57.

Al-Kaisi, MM and Broner, I. 2009. Crop water use and growth stages. *Crop series: Irrigation* 4.715:1-3.

Allen, RG, Pereira, LS, Raes, D and Smith, M. 1998. Crop evapotranspiration- Guidelines for computing crop water requirements, FAO Irrigation and drainage Paper No. 56. Food and Agricultural Organisation of the United Nations, Rome, Italy.

Allen, RG, Tasumi, M and Trezza, R. 2007. Satellite-based energy balance for mapping evapotranspiration with internalized calibration (METRIC)-Model. *Journal of Irrigation and Drainage Engineering* 133(4): 380-394.

Allen, RG, Pereira, LS, Howell, TA and Jensen, ME. 2011. Evapotranspiration information reporting: I. Factors governing measurement accuracy. *Agricultural Water Management* 98:899-920.

Bastiaanssen, WGM, Menenti, M, Feddes, RA and Holtslag, AAM. 1998. A remote sensing surface energy balance algorithm for land (SEBAL) 1. Formulation. *Journal of Hydrology* 212-213: 198-212.

Baviaans Tourism. 2012. The Baviaanskloof area. http://www.baviaans.co.za/page/information_baviaanskloof [Accessed: 10/10/2019].

Badola, A. 2009. Validation of Surface Energy Balance System (SEBS) over forest land cover and sensitivity analysis of the model. MSc. International Institute for Geo Information Science and Earth Observation Enschede, Netherlands.

Bowen, IS. 1926. The ratio of heat losses by conduction and by evaporation from any water surface. *Physical Review* 27:779-787.

Burger, C. 1999. Comparative evaporation measurements above commercial forestry and sugarcane canopies in the KwaZulu-Natal Midlands. Unpublished MSc. University of Natal, Pietermaritzburg, KwaZulu-Natal, South Africa.

Cook, DR. 2007. Energy balance Bowen ratio. In: *Energy Balance Bowen Ratio (EBBR) Handbook.* ARM TR-037. Illinois, USA.

Costa, M.H, Botta, A, Cardille, J.A, 2003. Effects of large-scale changes in land cover on the discharge of the Tocantins River, Southeastern Amazonia. *Journal of Hydrology* 283:206–217.

Courault, D, Seguin, B and Olioso, A. 2005. Review on estimation of evapotranspiration from remote sensing data: From empirical to numerical modelling approaches. *Irrigation and Drainage Systems* 19:223-249.

De Bruin, HAR, Van Den Hurk, BJJ and Kohsiek, W. 1995. The scintillation method tested over a dry vineyard area. *Boundary-Layer Meteorology* 76(1):25-40.

Dzikit, S, Jovanovic, NZ, Bugan, R, Israel, S and Le Maitre, DC. 2014. Measurement and modelling of evapotranspiration in three fynbos vegetation types.*Water SA* (40)2: 189-198.

Department of Water Affairs and Forestry (DWAF). 1999. Stream Flow Reduction Activities: Combined licensing and authorisation guidelines. Pretoria, South Africa.

Elhag, M, Psilovikos, A, Manakos, I and Perakis, K. 2011. Application of the Sebs water balance model in estimating daily evapotranspiration and evaporative fraction from remote sensing data over the Nile Delta. *Water Resource Manage* 1-12.

Engman, ET and Gurney, RJ. 1991. *Remote Sensing in Hydrology.* Chapman and Hall, London, United Kingdom.

Everson, CS. 2001. The water balance of a first order catchment in the montane grasslands of South Africa. *Journal of Hydrology* 241:110-123.

Everson, C, Clulow, A and Mengistu, M. 2009. *Feasibility study on the determination of riparian evaporation in non-perennial systems*. Report No. TT 424/09. Water Research Commission, Pretoria, RSA

Falkenmark, M, Andersson, L, Castensson, R, Sundblad, K, Batchelor, C, Gardiner, J, Lyle, C, Peters, N, Pettersen, B, Quinn, P, Rckström, J, Yapijakis, C, 1999. *Water: A reflection of land use*. Swedish Natural Science Research Council,Stockholm, Sweden.

French, AN, Jacob, F, Anderson, MC, Kustas, WP, Timmermans, W. Gieske, A, Su, Z, Su, H, McCabe, MF, Li, F, Prueger, J and Brunsell, N. 2005. Surface energy fluxes with the advanced spaceborne thermal emission and reflection radiometer (ASTER) at the

Iowa 2002 SMACEX site (USA). *Remote Sensing of Environment* 99:55-65.

Fritschen, LJ and Simpson. 1989. Surface energy and radiation balance systems: General description an improvements. *American Meteorological Society* 28:680-689.

Gibson, LA, Munch, Z and Engelbrecht, J. 2011. Particular uncertainties encountered in using a pre-packaged SEBS model to derive evapotranspiration in a heterogeneous study area in South Africa. *Hydrology and Earth System Sciences* 15:295-310.

Gibson, LA, Jarmain, C, Su, Z and Eckardt, FE. 2013. Estimating evapotranspiration using remote sensing and the Surface Energy Balance System − A South African perspective. *Water SA* (39)4: 477-484.

Google Earth. 2016. United States Department of State Geographer.

Gush, M. 2010. Assessing hydrological impacts of tree-based bioenergy feedstock. *Agricultural Water Management* 102:1-7. Gush, M. 2010. Assessing hydrological impacts of tree-based bioenergy feedstock. In ed. Amezaga, JM, van Maltitz, G and Boyes, S. *Assessing the Sustainability of Bioenergy Projects in Developing Countries: A framework for policy evaluation,* Ch. 3, 37-52. LAW Printing, RSA.

Gush, B and Dye, PJ. 2015. *Water use and socio-economic benefit of the biomass of indigenous trees Volume 2: Site specific technical report*. Report No. 1876/2/15. Water Research Commission, Pretoria, RSA.

Hill, RJ. 1992. Review of optical scintillation methods of measuring the refractive-index spectrum, inner scale and surface fluxes. *Waves in Random Media* 2:179-201.

Huang, C, Li, Y, Gu, J, Lu, L, Li, X. 2015. Improving estimation of evapotranspiration under water-limited conditions based on SEBS and MODIS data in arid regions. *Remote Sensing* 7:16795-16814.

Irmak, S. 2009. Crop coefficient values. [Internet]. University of Nebraska − Lincoln Extension, Lincoln, United States of America. Available from: http://www.ianrpubs.unl.edu/pages/publicationD.jsp?publicationId=1237. [Accessed: 26/03/15].

Jarmain, C, Everson, CS, Savage, MJ, Mengistu, MG, Clulow, AD, Walker, S and Gush, MB. 2009a. *Refining tools for evaporation monitoring in support of water resources management.* Report No. 1567/1/08. Water Research Commission, Pretoria, RSA.

Jarmain, C, Bastiaanssenm, W, Mengistu, MG, Jewitt, G and Kongo, V. 2009b. *A*

methodology for near-real time spatial estimation of evaporation. Report No. 1751/1/09. Water Research Commission, Pretoria, RSA.

Jewitt, GPW, Lorentz, SA, Gush, MB, Thornton-Dibb, S, Kongo, V, Wiles, L, Blight, J, Stuart-Hill, SI, Versfeld, D and Tomlinson, K. 2009. *Methods and guidelines for the licensing of SFRAs with particular reference to low flows*. Report No. 1428/1/09. Water Research Commission, Pretoria, RSA.

Jin, X, Guo, R and Xia, W. 2013. Distribution of actual evapotranspiration over Qaidam Basin, an arid area in China. *Remote Sensing* 5: 6976-6996.

Jovanovic, N and Isreal, S. 2012. Critical review of methods for the estimation of actual evapotranspiration in hydrological models. In: ed Irmak, A, *Evapotranspiration Remote Sensing and Modelling*, Ch. 15, 329-350. InTech, Rijeka, Croatia.

Knight, F. 2012. Agricultural Assessment of Baviaanskloof. Agri Informatics Development Trusts. Durbanville, South Africa.

Li, Z, Tang, R, Wan, Z, Bi, Y, Zhou, C, Tang, B, Yan, G and Zhang, X. 2009. A review of current methodologies for regional evapotranspiration estimation from remotely sensed data. *Sensors* 9:3801-3853.

Liou, YA and Kar, SK. 2014. Evapotranspiration estimation with remote sensing and various surface energy balance algorithms- A Review. *Energies* 7:2821-2849.

Ma, W, Hafeez, M, Rabbani, U, Ishikwa, H and Ma, Y. 2012. Retrieved actual ET using SEBS model from Landsat-5 TM data for irrigation area of Australia.

Mamo, TA. 2010. Estimation of actual evapotranspiration and water balance using combined geostationary and polar orbiting satellite products: A Case Study in Spain. MSc University of Twente – ITC, Enschede, 1-86.

Meijninger, WML and Jarmain, C. 2014. Satellite-based annual evaporation estimates of invasive alien plant species and native vegetation in South Africa. *Water SA* 40:95 108.

Meijninger, WML, Hartogensis, OK, Kohsiek, W, Hoedjes, JCB, Zuurbier, RM and De Bruin, HAR. 2002. Determination of area-averaged sensible heat fluxes with large aperture scintillometer over a heterogeneous surface- Flevoland field experiment. *BoundaryLayer Meteorology* 105:37-62.

Mengistu, MG, Everson, CS, Moyo, NC and Savage, MJ. 2014. *The validation of the*

variables (evaporation and soil moisture) in hydrometeorological models. Report No. 2066/1/13. Water Resource Commission, Pretoria, South Africa.

Mengistu, MG. 2008. Heat and energy exchange above different surfaces using Surface Renewal. Ph.D. thesis. University of KwaZulu-Natal, Pietermaritzburg, South Africa.

Mengistu, MG and Savage, MJ. 2010. Surface renewal method for estimating sensible heat flux. *Water SA* 36(1):9-18.

Meyers, TP and Baldocchi, DD. 2005. Current micrometeorological flux methodologies with applications in agriculture. *Micrometeorology in Agricultural Systems, Agronomy Monograph* 47:381-396.

Mkhwanazi, MM and Chavez, JL. 2013. Mapping evapotranspiration with the remote sensing ET algorithms METRIC and SEBAL under advective and non-advective conditions: accuracy determination with weighing lysimeters. *Hydrology Days* 1-6.

Moran, MS, Clarke, TR, Inoue, Y and Vidal, A. 1994. Estimating crop water deficit using the relation between surface-air temperature and spectral vegetation index. *Remote Sensing of Environment* 49(3): 246-263.

Mucina, L and Rutherford, MC. 2006. *The vegetation of South Africa, Lesotho and Swaziland.* Strelitzia 19. South African National Biodiversity Institute, Pretoria, South Africa.

National Aeronautics and Space Administration (NASA). 2010. *Landsat 7 science data user's handbook*. USA.

National Water Act (NWA). 1998. Act No. 36 of 1998. Government Printer, Pretoria, South Africa.

Paw U, KT and Brunet, Y. 1991. A surface renewal measure of sensible heat flux density.20th *Conference on Agricultural and Forest Meteorology*,52–53. American Meteorological Society Boston,USA.

Paw U, KT, Qiu, J, Su, HB, Watanabe, T, Brunet,Y. 1995. Surface renewal analysis: A new method to obtain scalar fluxes without velocitydata. *Agricultural and Forest Meteorology* 74: 119–137.

Ramoelo, A, Majozi, N, Mathieu, R, Jovanovic, N, Nickless, A and Dzikiti, S. 2014. Validation of the global evapotranspiration product (MOD16) using flux tower data in the African Savanna, South Africa. *Remote Sensing* 6:7406-7423.

Reynolds, O. 1895. On the dynamical theory of incompressible viscous fluids and the determination of the criterion. *Philosophical Transactions of the Royal Society of London* 186:123-164.

Rwasoka, DT, Gumindoga, W and Gwenzi, J. 2011. Estimation of actual evapotranspiration using the Surface Energy Balance System (SEBS) algorithm in the Upper Manyame catchment in Zimbabwe. *Physics and Chemistry of the Earth* 36: 736-746.

Savage, MJ, Everson, CS, Metelerkamp, BR. 1997. *Evaporation measurement above vegetated surfaces using micro-meteorological techniques.* Report No. 349/1/97. Water Research Commission Report, Pretoria, South Africa

Savage, MJ, Everson CS, Odhiambo GO, Mengistu MG and Jarmain C. 2004. *Theory and practice of evapotranspiration measurement, with special focus on SLS as an operational tool for the estimation of spatially-averaged evaporation.* Report No. 1335/1/04. Water Research Commission, Pretoria, South Africa.

Savage, MJ, Odhiambo, Mengistu, MG, Everson, CS and Jarmain, C. 2010. Measurement of grassland evaporation using a surface-layer scintillometer. *Water SA* 36(1):1-8.

Schulze, R.E. 2003. *Modelling as a Tool in Integrated Water Resources Management: Conceptual Issues and Case Study Applications*. Report No. 749/1/04 Water Research Commission, Pretoria, South Africa.

Schulze, RE and Pike, A. 2004. *Development and evaluation of an installed hydrological modelling system.* Report No. 1155/1/04. Water Research Commission, Pretoria, South Africa.

Schulze, R.E. 2007. Baseline Land Cover. *In:* Schulze, R. E. *South African Atlas of Climatology and Agrohydrology*. Report No.1489/1/06. Water Research Commission, Pretoria, South Africa.

Shoko, C, Clark, D, Mengistu, M, Dube, T and Bulcock, H. 2015b. Effect of spatial resolution on remote sensing estimation of total evaporation in the uMngeni catchment, South Africa. *Journal of Applied Remote Sensing*. 9:1-22.

Singh, KR and Senay, G. 2016. Comparison of four different energy balance models for estimating evapotranspiration in the Midwestern United States. *Water* 8(9):1-19.

Snyder, P, Spano, D and Paw U, KT. 1995. Surface renewal analysis for sensible and latent heat flux density. *Boundary-Layer Meteorology* 77:249-266.

Shuttleworth, WJ. 2008. Evapotranspiration measurement methods. SAHRA, Arizona, USA.

South African National Biodiversity Institute (SANBI). 2012. Vegetation map of South Africa, Lesotho and Swaziland. Available from: http://bgis.sanbi.org/SpatialDataset/Detail/18 [Accessed: 14 October 2016].

South African National Biodiversity Institute (SANBI). 2016. Vegetation of South Africa. Available from: http://pza.sanbi.org/vegetation [Accessed: 17 October 2016].

Su, Z. 2002. The surface energy balance system (SEBS) for estimation of turbulent heat fluxes. *Hydrology and Earth System Sciences* 6(1):85-99.

Swinbank, WC. 1951. The measurement of vertical transfer of heat and water vapour by eddies in the lower atmosphere. *Journal of Meteorology* 8(3):135-145.

Thiermann, V. and Grassl, H. 1992. The measurement of turbulent surface-layer fluxes by use of bichromatic scintillation.*Boundary-Layer Meteorology* 58:367-389.

Thoreson, B, Zwart, S, Bastiaanssen, W and Davds, G. (2004). Estimating actual evapotranspiration without land use classification. Water Rights and Related Water Supply Issues.

Tian, X, van der Tol, C, Su, Z, Li, Z, Chen, E, Li, X, Yan, M, Chen, X, Wang, X, Pan, X, Ling, F, Li, C, Fan, W and Li, L. 2015. Simulation of forest evapotranspiration using time-series parameterization of the Surface Energy Balance System (SEBS) over the Qilian Mountains. *Remote Sensing* 7:15822-15843.

United States Geological Survey (USGS). 2015. Landsat instruments. (http://landsat.usgs.gov/landsat8.php) [Accessed 20/06/2016].

Van der Tol, C and Parodi, GN. 2011. Guidelines for remote sensing of evapotranspiration. In:ed. Irmak, A, *Evapotranspiration- Remote Sensing and Modelling*, Ch. 11, 227 250. InTech, Rijeka, Croatia.

Van der Kwast, J, Timmermans, W, Gieske, A, Su, Z, Olioso, A, Jia, L, Elbers, J, Karssenberg, D and de Jong, S. 2009. Evaluation of the Surface Energy Balance System (SEBS) applied to ASTER imagery with flux-measurements at the SPARC 2004 site (Barrax, Spain). *Hydrology and Earth System Sciences* 13: 1337-1347.

Verstraeten, WW, Veroustraete, F and Feyen, J. 2008. Assessment of evapotranspiration and soil moisture content across different scales of observation. *Sensors* 8:70-117.

Wagner, W, Verhoest, NE, Ludwig, R and Tedesco, M. 2009. Remote sensing in hydrological sciences. *Hydrology and Earth System Sciences* 13:813-817.

Warburton, ML, Schulze, RE and Jewitt, GPW. 2010. Confirmation of ACRU model results

for applications in land use and climate change studies. *Hydrology and Earth System Sciences* 14:2399-2414.

Warburton, ML, Schulze, RE and Jewitt, GPW. 2011. Hydrological impacts of land use change in three diverse South African catchments. *Journal of Hydrology* 414 415:118-135.

Warburton, ML, Clulow, A, Van Rensburg, S, Bulcock, H, Jewitt, GPW, Everson, CE and Horan, MJC. 2014. Toward understanding the environmental change impacts on hydrological responses through long term monitoring: Reestablishment of the Cathedral Peak research catchments, South Africa.

Workineh, G, Berhan, G, Nedaw, D. 2016. Evaluation of Surface Energy Balance System (SEBS) model for estimation of evapotranspiration in Eastern Ethiopia. *Journal of Resources Development and Management* 25:52-59.

Zhang, L, Dawes, WR and Walker, GR. 2001. Response of mean annual evapotranspiration to vegetation changes at catchment scale. *Water Resources Research* 37: 701–708.

Zhuo, G, Ba. L, Ciren, P and Bu, L. 2014. Study on daily surface evapotranspiration with SEBS in Tibet Autonomous Region. *Journal of Geographical Sciences* 24(1): 113 128.